Journal of Sea Research 85 (2014) 379–394

Contents lists available at ScienceDirect

Journal of Sea Research

journal homepage: www.elsevier.com/locate/seares

Influence of environmental gradients on C and N stable isotope ratios in coral reef biota of the Red Sea, Saudi Arabia ☆

Benjamin Kürten [a,*], Ali M. Al-Aidaroos [b], Ulrich Struck [c], Hisham Sulaiman Khomayis [b], Waleed Yousef Gharbawi [b], Ulrich Sommer [a]

[a] GEOMAR Helmholtz Centre for Ocean Research Kiel, Marine Ecology (Food webs), Düsternbrooker Weg 20, 24105 Kiel, Germany
[b] King Abdulaziz University, Department of Marine Biology, Faculty of Marine Sciences, P. O. Box 80207, Jeddah 21589, Saudi Arabia
[c] Leibniz-Institut für Evolutions- und Biodiversitätsforschung, Museum für Naturkunde, Invalidenstraße 43, 10115 Berlin, Germany

ARTICLE INFO

Article history:
Received 18 October 2012
Received in revised form 12 July 2013
Accepted 13 July 2013
Available online 20 July 2013

Keywords:
Ecohydrography
Guild
Isoscapes
Latitudinal gradient
SIAR
Stable isotopes

ABSTRACT

The Red Sea features a natural environmental gradient characterized by increasing water temperature, nutrient and chlorophyll *a* concentrations from North to South. The aim of this study was to assess the relationships between ecohydrography, particulate organic matter (POM) and coral reef biota that are poorly understood by means of carbon ($\delta^{13}C$) and nitrogen ($\delta^{15}N$) stable isotopes. Herbivorous, planktivorous and carnivorous fishes, zooplankton, soft corals (Alcyonidae), and bivalves (*Tridacna squamosa*) were a priori defined as biota guilds. Environmental samples (nutrients, chlorophyll *a*), oceanographic data (salinity, temperature), POM and biota were collected at eight coral reefs between 28°31′ N and 16°31′ N. Isotopic niches of guilds separated in $\delta^{13}C$ and $\delta^{15}N$ isotopic niche spaces and were significantly correlated with environmental factors at latitudinal scale. Dietary end member contributions were estimated using the Bayesian isotope mixing model SIAR. POM and zooplankton ^{15}N enrichment suggested influences by urban run-off in the industrialized central region of the Red Sea. Both $\delta^{15}N$ and their relative trophic positions (RTPs) tend to increase southwards, but urban runoff offsets the natural environmental gradient in the central region of the Red Sea toward higher $\delta^{15}N$ and RTPs. The present study reveals that consumer $\delta^{13}C$ and $\delta^{15}N$ in Red Sea coral reefs are influenced primarily by the latitudinal environmental gradient and localized urban runoff. This study illustrates the importance of ecohydrography when interpreting trophic relationships from stable isotopes in Red Sea coral reefs.

1. Introduction

The Red Sea features a combination of natural and anthropogenic gradients of temperature, salinity and nutrients (Edwards, 1987). Primary production and nutrient concentrations gradually increase from North to South and toward the coasts, while variations of this trend can be attributed to the winter monsoon, production in coastal reefs, and run-off from urban settlements (Acker et al., 2008; Raitsos et al., 2013; Sofianos and Johns, 2007). Coral reefs provide a variety of ecosystem services including seafood, coastal protection, biogeochemical processes, recreational possibilities, and revenue through tourism (Jennings and Polunin, 1996; Moberg and Folke, 1999). The degree of biogeochemical activity can be greater at the fore reef and was related to the availability and utilization of ocean-derived macronutrients, which emphasized the consideration of dynamic oceanographic catchments for coral reefs with multiple intertwined mechanistic linkages (Furnas et al., 2005; Wyatt et al., 2010a, 2012a). Thus, as coral reef trophodynamics are governed by (regional) oceanographic conditions, they are also susceptible to climate change and ocean acidification at large spatial scales which potentially alter the quality and quantity of allochthonous food available to consumers in the adjacent coral reefs (Genin et al., 2009; Wyatt et al., 2010a; Yahel et al., 1998). Yet, relatively little is known about the biogeochemistry and trophodynamics of coral reefs in the Red Sea, and how these relate to spatial pattern observed in environmental drivers' at large spatial scales.

Stable isotope analysis (SIA) of the macronutrients carbon (^{13}C:^{12}C; $\delta^{13}C$) and nitrogen (^{15}N:^{14}N; $\delta^{15}N$) has often been used as a biogeochemical approach to the study of trophodynamics, because SIA provides time-integrated measures of an organism's feeding ecology, weighted by the elemental composition of the dietary items (Hobson, 1999; Hobson and Welch, 1992; Kaehler et al., 2000; Polunin et al., 2001). In general, stable isotope signatures vary within environmental substrates depending on earth system processes. The term ecohydrography summarizes the joint effects of geography, ecosystem, hydrographic regime and biogeochemistry. Ecohydrography therefore sets the framework for and leads to the development of isoscapes

☆ Disclosure: BK conceived the study, carried out field work, stable isotope analyses and data evaluation. AA identified and sorted zooplankton and provided logistical support during the expedition. HK assisted in the collection of water and plankton samples. WG participated in the collection of macrofauna. USt carried out POM stable isotope analyses. BK wrote the manuscript. USo, USt, AA and HK provided editorial advice. The authors declare that they have no conflict of interest.

* Corresponding author. Tel.: +49 431 600 4016; fax: +49 431 600 4402.
E-mail address: kuertenb@googlemail.com (B. Kürten).

1385-1101/$ – see front matter © 2013 Elsevier B.V. All rights reserved.
http://dx.doi.org/10.1016/j.seares.2013.07.008

(isotopic geographic patterns). Isoscapes potentially reveal long-term integration patterns of spatial variances in environmental conditions and biological influences (Bowen, 2010; Jennings and Warr, 2003; McMahon et al., 2013). Isoscapes are informative about the combined effects of the underlying bionomic and scenopoetic processes that govern, for example, the δ^{13}C and δ^{15}N values of biota relative to large-scale environmental controls (Hill and McQuaid, 2008; Newsome et al., 2007).

Metabolic reactions that discriminate against the heavier isotopes lay the foundation for the trophodynamic approaches, as more positive δ^{13}C and δ^{15}N values [‰] usually point toward a higher trophic level of a consumer relative to its diet. Trophic enrichment factors (TEFs; denoted Δ) are commonly used to describe the difference in ‰ between sources and consumers across adjacent trophic levels and usually range from 2 to 4‰ for δ^{15}N and 0.5–1‰ for δ^{13}C (McCutchan et al., 2003; Post, 2002; Sweeting et al., 2007). Due to the smaller Δ, values of δ^{13}C are generally useful in tracing C fluxes, whereas δ^{15}N conveys information of the relative trophic position (RTP) of consumers in a continuously measurable unit when isotope ratios of dietary sources are known (Post, 2002; Vander Zanden et al., 1997). In δ^{13}C and δ^{15}N biplots (δ-space) the isotopic niche widths of biota are descriptors of and frequently align with ecological niches that can be inferred, for example, from gut content analyses (Bearhop et al., 2004; Layman et al., 2007, 2012). To supplement the descriptive assessment of trophodynamics with quantitative rigors, source partitioning mixing models that incorporate isotopic mass-balances, such as IsoSource (Phillips and Gregg, 2003) and the more recent Bayesian variant SIAR (Parnell et al., 2010), have been developed and allow constraining the isotopic source contributions by dietary end members (Layman et al., 2012). In fact, the SIAR model can be applied to underdetermined systems that infringe the 'point-in-polygon' assumption of non-Bayesian linear mixing models, because SIAR incorporates variance in parameters such as TEFs in an additional error term, and propagates sources of uncertainty into posterior probability distributions (Parnell et al., 2010).

Spatial variations of δ^{13}C and δ^{15}N of biota at the base of food webs potentially indicate characteristic features of ecosystems and set the basis for the configuration of food webs i.e. in relation to the availability of nutrients and stoichiometric ratios thereof (Sommer et al., 2002). However, considered separately, the evaluation of δ^{13}C or δ^{15}N values offers also interpretations about the isotopic macronutrient end members (if more than one). The δ^{13}C, for instance, can provide clues about the principle C sources for primary producers and adjacent trophic levels, because the fractionation during C fixation of marine phytoplankton by RuBisCO depletes their δ^{13}C values up to -27‰, whereas the δ^{13}C of internal bicarbonate (HCO_3^-) pools in coral tissue and their zooxanthellae tends to be ^{13}C enriched up to -7‰ and -11.7‰, respectively (Marshall et al., 2007; Muscatine et al., 1989). The δ^{13}C values of biota are therefore potentially useful to distinguish between pelagic and reef-derived end members (e.g. Fry et al., 1982). The analysis of N isotopes also conveys source information. Depleted δ^{15}N values in biota were, for instance, attributed to either utilization of N_2 fixation (Alamaru et al., 2009; Lesser et al., 2007; Minagawa and Wada, 1984; Peterson and Fry, 1987), atmospheric deposition (Aberle et al., 2010; Wankel et al., 2010), or mangrove habitats (Fogel et al., 2008). Moreover, the ^{15}N enrichment of corals was also interpreted as an indicator of sewage-derived organic matter input (Marion et al., 2005), including reefs off Jeddah (Risk et al., 2009a,b). Though, despite the large potential of the SIA approach to assess macronutrient end members and trophodynamics in coral reefs, the few existing studies using SIA focused mainly on coral reef fishes or selected coral species (e.g. Carassou et al., 2008; Frédérich et al., 2009; Fry et al., 1982; Greenwood et al., 2010; Heikoop et al., 2000; Wyatt et al., 2010b). However, regarding nutrient fluxes and trophodynamics recent studies indicate complexity at inter-reef spatial scales, e.g. the relative importance of oceanic vs. reef-based resources for carnivorous, herbivorous and planktivorous fishes (Wyatt et al., 2012b), the availability and function of coral mucus as a vector for macronutrients (Naumann et al., 2009; Wild et al., 2004), or the mediation of nutrient fluxes by sponges (Slattery et al., 2013; van Duyl et al., 2011).

Here, we describe the δ^{13}C and δ^{15}N isotope values of particulate organic matter (POM), zooplankton and a range of biota collected in coral reefs along the coast of Saudi Arabia across a large spatial-scale environmental gradient featured by the Red Sea. We defined ecological guilds a priori and then collected potentially corresponding species including *Tridacna squamosa* (Bivalvia), soft coral (Alcyonidae), zooplankton, as well as herbivorous, planktivorous and carnivorous fishes. We explore whether changes in environmental variables (nutrients, chlorophyll *a*) alter δ^{13}C and δ^{15}N values and propagate from primary consumers to higher trophic levels. It was hypothesized that variation in ecohydrography at latitudinal scale would alter RTPs and trophodynamics as indicated by C and N SIA within the Red Sea isoscape.

2. Materials and methods

2.1. Study area

The Red Sea is a narrow shelf sea with limited hydrographic connections to water bodies other than the Indian Ocean (Edwards, 1987). The winter monsoon across the region and high evaporation of the Red Sea results in the intrusion of nutrient rich water from the Gulf of Aden and the adjacent Arabian Sea through the strait of Bab-al-Mandab in the South and which enhances primary production within its reach (Acker et al., 2008; Raitsos et al., 2013; Sofianos and Johns, 2007). Utilization of nutrients by primary producers decreases the concentration of nutrients toward the North and leads to oligotrophic conditions in the northern Red Sea and the Gulf of Aqaba (Edwards, 1987). Although the Red Sea receives generally limited terrestrial run-off local point sources of pollution include wastewater from urban settlements, aquaculture, industrial activities, and maritime activities (Abu-Hilal and Al-Najjar, 2009; Khalaf and Kochzius, 2002; Mohamed and Al-Shehri, 2012; Risk et al., 2009b).

2.2. Sample collection

The samples for this study were collected in autumn from mid-September to mid-October 2011 at fringing-type coral reefs along the coast of Saudi Arabia across a latitudinal distance of ~1500 km (Fig. 1, Table 1). The expedition took place during the initiation period of the phytoplankton succession at the beginning of autumn, which is considered to be triggered by convective vertical mixing of cold and nutrient rich waters (Raitsos et al., 2013). The eight sampling sites were assigned to three meridional regions. The coral reef sites in the North are characterized by steep coral walls, very oligotrophic conditions, and relatively pristine conditions with negligible anthropogenic impact [1) Maqna in the Gulf of Aqaba and 2) Al Wajh (Reja Island)]. The central region is exposed to industrial activities and to urban run-off [3) Yanbu, 4) Mastoura, 5) Jeddah]. The sites in the South [6) Al Lith, 7) Doga, 8) Farasan] cover the spatial extent of the Farasan Banks. The Farasan archipelago is situated at the southern end of the Farasan Banks where mesotrophic conditions prevail. The sampling location Farasan was situated at a small coral island 14 km southwest off Farasan Island.

Besides sampling for environmental data, we a priori defined feeding guilds and collected potentially corresponding animals including Bivalvia, soft coral, zooplankton, and fishes for δ^{13}C and δ^{15}N stable isotope analysis (SIA). We consider seasonal variability to be negligible over spatial variability, because all sites were sampled within a period of five weeks. The selection of taxa was subject to presence and catchability in the field. The guild classifications for invertebrates were: (I) zooplankton, (II) Bivalvia (fluted giant clam, *Tridacna squamosa*), and (III) soft coral (*Sinularia* sp. and *Sarcophyton* sp.; Alcyoniidae). Fish guilds included: (IV) herbivores (surgeonfish, *Acanthurus sohal*, *Ctenochaetus*

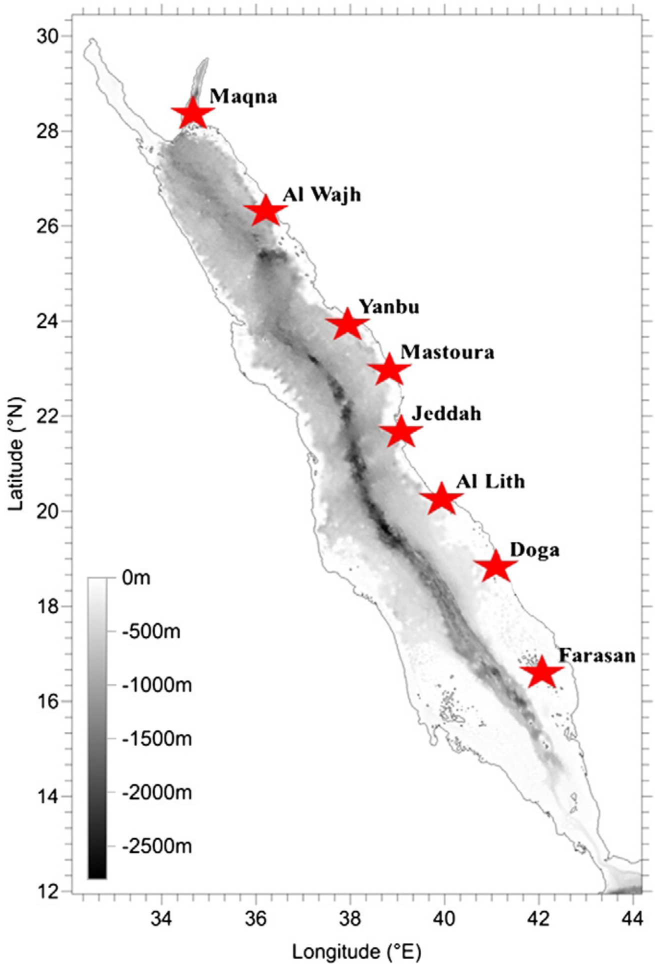

Fig. 1. Bathymetric chart of the Red Sea indicating sampling sites at the coast of Saudi Arabia. Refer to Table 1 for geographic position.

striatus), (V) planktivores (scissortail sergeant, *Abudefduf sexfasciatus*), and (VI) carnivores (halfspotted grouper, *Cephalopholis hemistiktos*). Assignments of fish taxa to guilds were verified using FishBase (Froese and Pauly, 2013).

2.3. Environmental sample collection

Salinity and temperature were determined at 10 m depths using a conductivity, temperature, depth sensor (CTD; Sea-Bird MicroCAT SBE37-SM, USA). Seawater was collected at the same time from 10 m depth using a peristaltic pump (Ismatech ECOLINE VC-380, FRG) and Tygon® tubing. The bulk of the collected seawater for the filtration of suspended particulate organic matter (POM) was screened through 50 µm mesh to remove larger zooplankton and collected in cooled and shaded folding canisters. Water samples were also collected for the analysis of nutrients but not screened and collected in Nalgene® bottles which were kept in a cooler on ice until further processing. Ashore, seawater for the analysis of dissolved silicate (Si) was filtered through 0.2 µm Nuclepore™ polycarbonate filter (Whatman, UK). Aliquots of seawater for total N (TN) and total P (TP) analysis were neither screened nor filtered. Aliquots were collected in triplicates and stored frozen in scintillation vials at −20 °C during expedition and at −80 °C in the laboratory. During filtrations of POM, known volumes of water were added until clogging of the filter (pigments: 15–28 L; SIA: 5–12 L). POM was collected in triplicates on pre-combusted (4 h, 450 °C) 47 mm GF/F (Whatman, UK) for determinations of pigment concentrations by HPLC (here, only chlorophyll *a* data are reported; henceforth 'chl *a*'). Filters for pigment analysis were wrapped in aluminum foil and stored in liquid N_2 during the expedition and at −80 °C at the laboratory. Another six replicates of POM were collected on pre-combusted 25 mm GF/F for δ^{13}C and δ^{15}N SIA. Filters for SIA were oven dried at 50 °C and stored in desiccators.

2.4. Zooplankton collection

Zooplankton tows were carried out at noon and midnight using a Bongo net (Hydro-Bios, FRG; opening diameter = 60 cm, 55 µm mesh size, non-filtering cod ends). The net was geared to remain submerged at 10–15 m depths and towed horizontally parallel to the reef front (30 min at ~1 kn), crossing several times the position where seawater and POM were collected. Ashore, zooplankton was sorted live to the lowest practical taxonomic level. In total 378 zooplankton samples were prepared for SIA mostly at the genus and species level and included herbivorous, omnivorous and carnivorous Copepoda, raptorial predators (Chaetognatha) and a complex of zoea larvae (Decapoda). Giving enough time (1–2 h) for gut evacuation, 1–150 specimens per SIA sample – depending on size and availability – were transferred into pre-weighed tin capsules (HEKAtech, FRG), oven dried (24–48 h, 50 °C) and stored in desiccators prior to SIA. Acidifications prior to SIA of whole zooplankton were avoided. Although several studies revealed significant changes in the δ^{13}C and δ^{15}N values of whole animals after acidification attributable to their carbonate content (e.g. Bunn et al., 1995; Carabel et al., 2006), δ^{13}C and δ^{15}N values of taxa with low carbonate content are comparable among studies regardless of prior acidification (Bosley and Wainright, 1999; Kolasinski et al., 2008; Soreide et al., 2006). Here, most zooplankton taxa possessed an exoskeleton, and subjecting invertebrates with low carbonate content to acidification effectively introduces a larger error to the obtained isotopic signatures than possibly caused by traces of carbonates in the exoskeletons (Mateo et al., 2008). De Lecea et al. (2011), for example, showed no acid treatment effects on zooplankton isotopic signatures for *Undinula vulgaris* (Calanoida), a species which was frequently sampled in the present study. In fact, as the exoskeleton is composed of C and N of mainly dietary origin, fractions of their δ^{13}C and δ^{15}N may therefore be of some interest as food web tracer (Mateo et al., 2008).

Table 1
Geographic position and biological–oceanographic characteristics at eight sampling sites along the Saudi Arabian Red Sea coast (chlorophyll *a*: HPLC measurements; total N (TN), total P (TP) and dissolved Si; chlorophyll *a* and nutrient data: all n = 3).

Site	Geographic position		Temperature		Salinity		Chl *a* [ng L−1]		TN [µmol L−1]		TP [µmol L−1]		Si [µmol L−1]	
	Latitude [N]	Longitude [E]	Mean [° C]	±SD	Mean	±SD	Mean	±SD	Mean	±SD	Mean	±SD	Mean	±SD
Maqna	28°31′	34°47′	26.7	0.0	40.92	0.3	145	2	3.1	0.1	0.1	0.0	0.8	0.1
Al Wajh	26°10′	36°21′	28.9	0.8	40.38	0.1	97	17	3.3	0.1	0.1	0.0	0.8	0.1
Yanbu	23°51′	37°59′	28.5	0.1	39.66	0.2	220	8	3.8	0.1	0.2	0.0	0.8	0.1
Mastoura	23°06′	38°45′	30.3	0.2	39.81	0.0	259	48	3.1	0.1	0.2	0.0	0.5	0.0
Jeddah	21°41′	38°59′	29.3	0.6	39.44	0.6	233	11	3.2	0.0	0.2	0.0	0.7	0.1
Al Lith	20°10′	39°52′	30.6	0.9	39.18	0.2	748	57	4.1	0.1	0.2	0.0	0.4	0.0
Doga	19°35′	40°37′	29.9	1.5	39.08	0.3	526	30	3.5	0.1	0.2	0.0	0.5	0.0
Farasan	16°31′	42°07′	32.0	0.1	38.08	0.4	3416	238	5.1	0.1	0.5	0.0	1.2	0.0

2.5. Macrofauna collection

Macrofauna were collected by SCUBA diving between 5 and 15 m depths at the seaward reef slopes. Within-sites, potential small spatial scale variability in resource utilization and connectivity to the oceanic domain as evidenced by the isotopic signatures of consumers cannot be negated, but seems negligible when compared to the large-scale ecohydrographic gradients described in the present study (c.f. Hill and McQuaid, 2008; Slattery et al., 2013; Wyatt et al., 2012a). Fish were collected using nets and baited traps. We aimed at the collection of at best ten specimens per species, but availability in the field prevented some taxa being collected from all sites, with a list presented in Table A.1 (Online Resource). In total 214 fish, 64 bivalve and 21 soft coral samples were collected. The tissue types used for SIA were dorsal white muscle tissue for fish and adductor muscle for *T. squamosa*. Soft coral tissues from several colonies per taxon were pooled. Only similar-sized adult animals were dissected and approx. 1–2 g of tissue removed. Tissue plugs were transferred into Eppendorf tubes, oven dried (24–48 h, 50 °C), and ground to fine powder using pestle and mortar. Aliquots of approximately 0.5–0.8 mg per sample were weighed (Elementar, FRG) and stored in desiccators pending SIA.

2.6. Chlorophyll a analysis

Pigments were extracted and measured via high-performance liquid chromatography (HPLC). For extraction, filters and cells were disrupted with glass pearls on a cooled bead beater and the pigments extracted with acetone. Supernatants were analyzed via HPLC and separated in a Varian Microsorb-MV column (100-3, C8, 100 × 4.6 mm) with 70% MeOH/30% 1 M NH_4-acetate and 100% MeOH as eluents. Pigments were identified and quantified using both a fluorescence detector (Waters 474 Scanning Fluorescence Detector, Waters GmbH, FRG) and a photodiode array absorption detector (Waters 2996 Photodiode Array Detector) after calibration with commercially available standards. The present study uses only the chl *a* data.

2.7. Nutrient analysis

TN, TP and Si of seawater samples were determined in triplicates according to the methods described in Grasshoff et al. (1999). Analysis was performed using a spectrophotometer (U-2900, Hitachi High-Technologies Europe, FRG). The trophic state of an aquatic ecosystem can only be characterized by TN or TP, because fractions of it (e.g. PON, POP, DIN, DIP) result from temporally highly variable fractionation of the total amount—i.e. POP and PON are large fractions of TP and TN during phytoplankton peaks and small fractions during seasonal biomass minima. In fact, as phytoplankton growth, pelagic grazing and remineralization rates are very rapid in coral reefs, this rapid uptake keeps stocks of dissolved inorganic nutrients within a relatively narrow range of low concentrations (Furnas et al., 2005). While this is not always appreciated in the oceanographic literature, it has become consensus during the extensive OECD-study on lake eutrophication (Vollenweider and Kerekes, 1982). Using TN and TP may be the preferable approach to assess the nutrient inventory and the trophic state of regional subsections of the Red Sea at large spatial scales (Downing, 1997).

2.8. Bulk $\delta^{13}C$ and $\delta^{15}N$ isotope analysis

Filters were randomly assigned to two sets of filters; one set was exposed to HCl fumes in a glass desiccator for 24 h to remove inorganic carbonates prior to bulk C SIA. Filters for N SIA were not acidified. SIA of animal samples were carried out using a varioISOTOPE cube (Elementar, FRG) elemental analyzer (EA) in CN mode connected to an IsoPrime100 (IsoPrime, UK) isotope ratio mass spectrometer (IRMS; King Abdulaziz University, KSA). Isotope ratios were expressed in conventional δ notation as a measure of heavy to light isotope using the equation: $\delta X\ (‰) = [(R_{Sample}:R_{Standard}) - 1] \times 10^3$, where δX is ^{13}C or ^{15}N, and R is the ^{13}C:^{12}C or ^{15}N:^{14}N ratio. Triplicates of internal reference material acetanilide #1 (Merck, FRG) were analyzed after every 10th unknown sample. Calibration of acetanilide #1 was carried out against IAEA reference materials (IAEA-N-1, IAEA-N-2 for $\delta^{15}N$; IAEA-CH-3, IAEA-CH-6, IAEA-CH-7 for $\delta^{13}C$). Stability of the instrumentation, analytical precision, drift correction and linearity were calculated from the repetitive analysis of acetanilide #1. The standard deviation for acetanilide #1 was 0.1‰ for $\delta^{13}C$ and 0.2‰ for $\delta^{15}N$. As a second internal standard reference material acetanilide #2 (Schimmelmann et al., 2009) was measured as first and last 'unknown' sample in each analytical batch sequence. Acetanilide #2 was measured with a $\delta^{13}C$ signature of −29.53‰ and $\delta^{15}N$ of 1.32‰. SIA of POM filters were carried out on a ThermoElectron Delta V IRMS (Humboldt-Universität zu Berlin, FRG). Peptone standards with known isotopic composition (N-content 11%; C-content 44%; $\delta^{15}N$ 7.6‰; $\delta^{13}C$ −14.3‰) were used after every 5th unknown sample and calibrated with IAEA-N-1 and IAEA-N-2 once a month. Stability of the instrumentation, analytical precision, drift correction and linearity performance were calculated from the repetitive analysis of the peptone standard. The standard deviation for replicate Peptone samples was <0.2‰ for both isotopes.

2.9. Data analysis

Correlations between environmental data and SIA results were evaluated using Pearson's correlation coefficients (SPSS 21.0). Unconstrained linear gradient ordination was used to display the Euclidian distances between sites based on linear correlations between biota isotope ratios and environmental variables following Lepš and Šmilauer (2003) using Canoco5. Stoichiometric ratios of nutrients (TN:TP, TN:Si, TP:Si) were added to the environmental variables. Data were transformed into a Euclidean dissimilarity matrix prior to Principal Component Analysis (PCA). The species-environment biplot diagram summarizes the effects of environmental descriptors upon isotopic ratios of reef biota; guild classifications were passively projected into the resulting ordination space. Linear regression models of environmental factors and $\delta^{13}C$, $\delta^{15}N$ and RTP as dependent variables were used to constrain the influence of factors as indicated by PCA (SPSS 21.0).

Long-lived primary consumers, such as filter-feeding Bivalvia are good temporal integrators of the isotopic variation at the base of pelagic and benthic food webs (Post, 2002). Following Post (2002) we chose the Bivalvia *Tridacna squamosa* as baseline organisms, a conspicuous species in the Red Sea coral reefs. Based on *T. squamosa*, we calculated the relative trophic positions (RTPs) of other biota following equation 1: $RTP = [(\delta^{15}N_{Biota} - \delta^{15}N_{Tridacna}):3] + 1.5$. To account for its mixotrophy, the RTP of *T. squamosa* was set to 1.5, because *T. squamosa* relies for its nutrition on autotrophy performed by endosymbiotic zooxanthellae (trophic level 1) and heterotrophic feeding (trophic level 2) on plankton particles (Jantzen et al., 2008; Klumpp et al., 1992). In fact, zooxanthellae in *T. squamosa* assimilate ammonium-N from seawater and their nitrogenous end-products contribute to the diet of its host (Hawkins and Klumpp, 1995). Hence, for each studied reef *T. squamosa* integrates the N source isotope ratios it has been exposed to (as a mixture of dissolved N and of small-sized phytoplankton) over a relatively long period of time. Unfortunately, no *T. squamosa* were collected at Farasan and a mean $\delta^{15}N$ value of specimens collected at Al Lith and Doga was used instead. Pairwise comparison by two-way ANOVA examined differences between RTPs and $\delta^{13}C$ values using guild and site as factors. Levene's test of variance homogeneity confirmed ANOVA assumptions. One-way ANOVA was followed by Tukey's post hoc test. The contour plot of RTP, latitude and $\delta^{13}C$ used Natural Neighbor Interpolation (NNI; OriginPro 8) which interpolated RTP from a set of known points with points computed as weighted averages of the natural neighbors.

The Bayesian mixing model SIAR 4.1 (Parnell et al., 2010; R Development Core Team, 2013) was used to estimate the contribution of macronutrient sources to the diet of fishes. Separate SIAR runs were computed for each region (North, Central, and South). For each run we defined three matrices. The consumer matrix contained $\delta^{13}C$ and $\delta^{15}N$ values of *Cephalopholis hemistiktos* (carnivorous), *Acanthurus sohal* and *Ctenochaetus striatus* (herbivorous), and *Abudefduf sexfasciatus* (planktivorous). The source matrix contained averaged ($\pm$SD) $\delta^{13}C$ and $\delta^{15}N$ values of 'POM' and 'zooplankton'; the third source was denoted by 'reef' and used an average of the Bivalvia and soft corals $\delta^{13}C$ and $\delta^{15}N$ values. Initially we entered Bivalvia and soft corals as separate sources. But, as indicated by strong negative correlations between these two in diagnostic matrix plots included in SIAR, that explore the covariance between pairs of sources, we combined both sources and the SIAR model runs were repeated. The third matrix contained the trophic enrichment factors (TEFs) adapted from Wyatt et al. (2010b). The TEFs for 'zooplankton' were 3.2 $\pm$ 0.2‰ for $\delta^{15}N$ and 2.2 $\pm$ 1.0‰ for $\delta^{13}C$, for 'reef' 1.67 $\pm$ 0.4‰ for $\delta^{15}N$ and 1.3 $\pm$ 0.3‰ for $\delta^{13}C$. For 'POM' we used the average TEF of 2.4 $\pm$ 1.0‰ for $\delta^{15}N$ and 1.3 $\pm$ 0.3‰ for $\delta^{13}C$ as shown by Wyatt et al. (2010b). Elemental concentration dependencies were set to zero.

3. Results

3.1. Environmental parameters

From Maqna to Farasan temperature and phytoplankton biomass (proxy chl *a*) increased from 26.7 °C and 145 ng chl *a* L^{-1} to 32 °C and 3416 ng chl *a* L^{-1}, respectively (Fig. 2, Table 1; all CTD data from 10 m depths). Salinity decreased concomitantly from 40.92 to 38.08 PSU. Significant correlations (Pearson's *R*) of latitude with environmental factors such as salinity, chl *a* and temperature were observed (Table 2). The multivariate analysis showed that TN:TP and PSU were the most important environmental parameters best correlated with the distribution of isotope ratios and sites, whereas TN and TP itself were less important Eigenvectors (Fig. 3). Separation (in Euclidian space) of Al Lith and Doga from the other sites were positively correlated with the TN:Si ratios, whereas the approximation of the arrow for POM and the position in the ordination plot of the site Jeddah indicated a strong separation by isotope ratios. In fact, relatively depleted $\delta^{15}N$ values of POM were observed at Maqna, Al Lith and Doga, whereas POM was more ^{15}N enriched in the central Red Sea; the largest ^{15}N enrichment of POM was measured at Jeddah and at Farasan (Fig. 4). The output of the PCA was followed-up by one-way ANOVAs and linear regression models using bulk $\delta^{13}C$, $\delta^{15}N$, and RTPs as dependent variables and additional univariate constraint. The linear models for $\delta^{13}C$ and $\delta^{15}N$ were both significant ($p < 0.0002$ and $p < 0.0001$, respectively), although the predictive power of the model was relatively low for $\delta^{13}C$ ($R^2 = 0.052$), but higher for $\delta^{15}N$ ($R^2 = 0.345$). Environmental variables significantly influenced $\delta^{13}C$ and $\delta^{15}N$ values (one-way-ANOVA; $\delta^{13}C$: $F_{(8,668)} = 4.550$, MSE = 38.351, $p < 0.0001$; $\delta^{15}N$: $F_{(8,668)} = 43.938$, MSE = 194.772, $p < 0.0001$). TN, Si and TN:Si exhibited the largest influence, on $\delta^{15}N$, whereas $\delta^{13}C$ was significantly influenced mainly by latitude (Table 3). TP and TP:Si ratios were non-significant factors at $p < 0.05$. RTPs were most significantly influenced by chl *a*, latitude and PSU but not by Si, TN:TP and TN:Si (one-way-ANOVA,

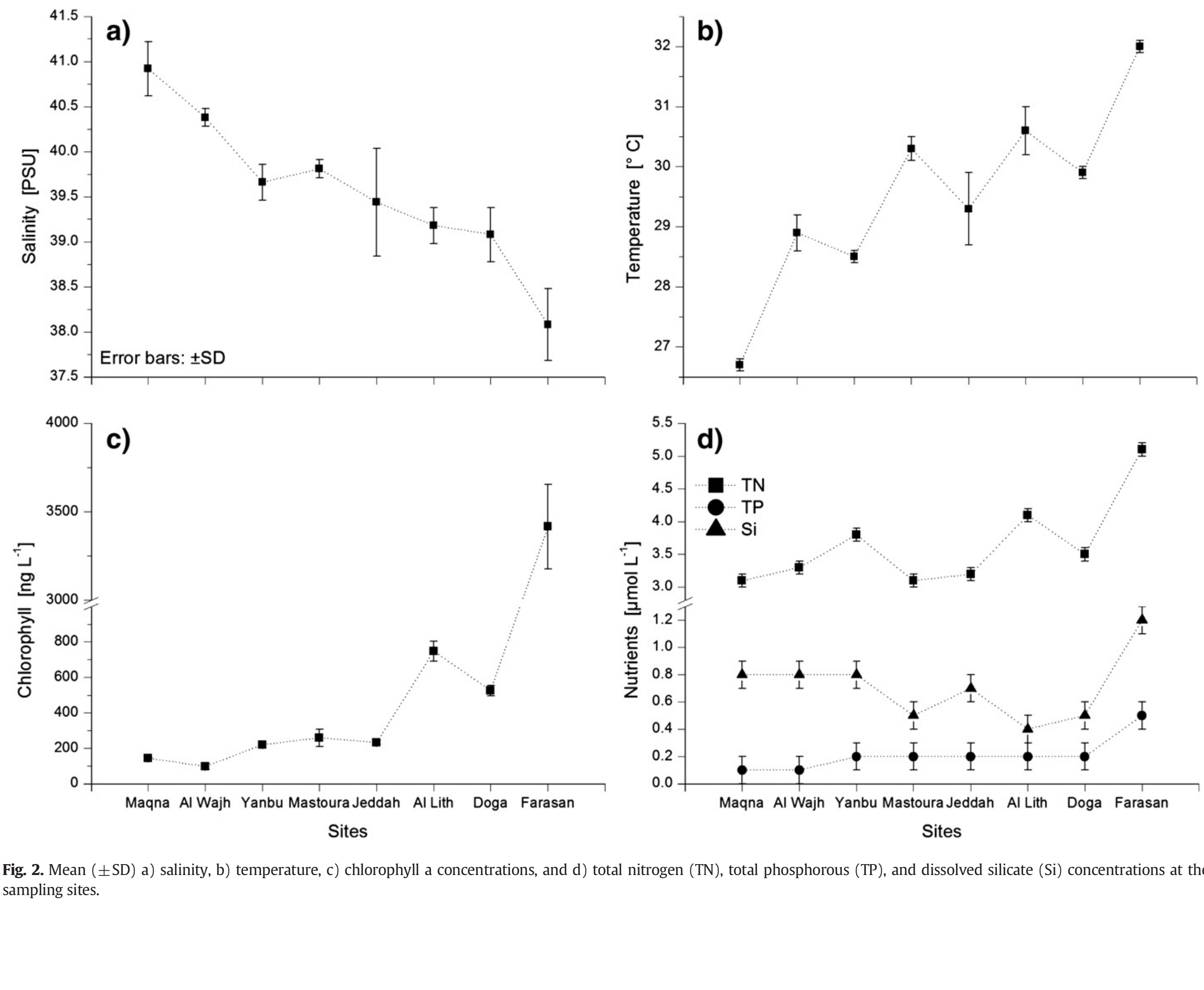

Fig. 2. Mean ($\pm$SD) a) salinity, b) temperature, c) chlorophyll a concentrations, and d) total nitrogen (TN), total phosphorous (TP), and dissolved silicate (Si) concentrations at the sampling sites.

Table 2
Summary of Pearson's correlation (*R* statistics) between latitude, environmental variables and $\delta^{13}C$ and $\delta^{15}N$ values of particulate organic matter (POM).

	Variable									
	Latitude	Temperature	Salinity	Chl *a*	TN	TP	Si	TN:TP	$\delta^{13}C$	$\delta^{15}N$
Latitude	1	−0.900	0.988	−0.758	−0.771	−0.830	−0.220	0.831	−0.103	−0.548
Temperature	**	1	−0.909	0.760	0.732	0.810	0.203	−0.630	0.136	0.513
Salinity	**	**	1	−0.816	−0.832	−0.891	−0.334	0.838	−0.093	−0.554
Chlorophyll	**	**	**	1	0.908	0.961	0.687	−0.625	0.103	0.441
TN	**	**	**	**	1	0.882	0.604	−0.592	0.103	0.439
TP	**	**	**	**	**	1	0.645	−0.771	0.087	0.510
Silicate	**	**	**	**	**	**	1	−0.222	0.028	0.182
TN:TP	**	**	**	**	**	**	**	1	−0.002	−0.503
$\delta^{13}C$	**	**	*	**	**	*	n.s.	n.s.	1	0.309
$\delta^{15}N$	**	**	**	**	**	**	**	**	**	1

n.s. = not significant.
* $p < 0.01$.
** $p < 0.05$.

$F_{(8,668)} = 26.539$, MSE = 12.632, $p < 0.0001$; linear model $R^2 = 0.232$, $p < 0.0001$; Table 3).

3.2. Stable isotope analysis

Averaged across all sites a priori defined guilds alone explained 47.6% of variance of RTPs (one-way-ANOVA, $F_{(6,697)} = 289.157$, $p < 0.0001$; linear model $R^2 = 0.476$, $p < 0.0001$). Most guilds occupied significantly discrete δ-spaces ($p < 0.001$; Tukey's HSD), but there were no differences in RTPs between POM and zooplankton and between Bivalvia and soft corals ($p < 0.963$ and $p < 0.991$; Tukey's HSD, Fig. 5). Nevertheless, separation in δ-space can be assumed for POM and zooplankton as well for Bivalvia and soft corals due to their $\delta^{13}C$ signatures (one-way-ANOVA, $F_{(6,697)} = 188.504$, $p < 0.0001$; Tukey's HSD, $p < 0.0001$, $p < 0.024$ respectively; Fig. 5). The $\delta^{13}C$ and $\delta^{15}N$ biplots are shown for each site (Fig. 6). Most ^{15}N (mean ± SD) depleted biota were *T. squamosa* at Maqna (0.3 ± 0.5‰) and soft corals at Al Wajh (0.8 ± 1.9‰), whereas carnivores were most ^{15}N enriched at Farasan (10.4 ± 0.4‰; Fig. 6; additional information in Table A.1 [Online Resource]). Among the herbivores, the most ^{15}N enriched *S. striatus* were collected at the coast of Jeddah (7.9 ± 0.2‰; Fig. 6). POM attained most ^{13}C depleted signatures in the northern Red Sea at Al Wajh and Yanbu (−24.2 ± 1.1‰ and −23.4 ± 1.2‰, respectively), while herbivores at Mastoura showed with −12.2 ± 0.3‰ the most enriched $\delta^{13}C$ (Fig. 6). Two-way ANOVA showed that region and guild significantly affected $\delta^{13}C$ and RTPs (Table 4), however, pairwise comparisons revealed no significant differences in RTPs between POM and herbivores from the central and southern region, and between carnivores from the northern region compared to the central and southern region of the Red Sea (Table 5). Mean (±SD) RTPs, $\delta^{13}C$, and $\delta^{15}N$ values for each region and guild are presented in Table 6.

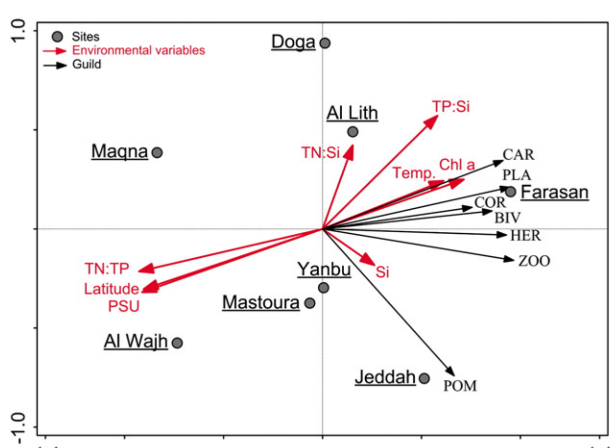

Fig. 3. Principal component analysis (PCA) of $\delta^{13}C$ and $\delta^{15}N$ values and environmental variables. Arrows for environmental variables point in the direction of the steepest increase of environmental variable values. Distances between the site symbols approximate the dissimilarity of isotopic signatures in Euclidean space. Guild classification arrows were passively projected a *posteriori* into the resulting ordination space and arrows point in the direction of the steepest increase of the isotopic values. The angle between arrows indicates the sign of the correlation between guilds. The length of the arrows resembles a measure of fit (PC axis 1 = 75.3%, PC axis 2 = 10.8%).

3.3. Red Sea isoscape

From North to South RTPs tend to increase with increasing temperature and chl *a* concentration, of which the latter two were inversely correlated with salinity (Table 2, Figs. 2, 3, 7).

The evaluation of $\delta^{13}C$ values allows the relative attribution of a consumer to its dietary end members (reef vs. oceanic). Across the whole scale range of $\delta^{13}C$ values of the present study, RTPs were significantly lower in the northern Red Sea as compared to the other two regions, and increased in the central region (Table 6, Fig. 7). The designation of sites to three regions of contrasting ecohydrography appeared conclusive and is apparent within the Red Sea isoscape (Fig. 7). The differences in frequency distribution strengthen this overall perception (Fig. 7b). Indeed, animals with relatively depleted $\delta^{13}C$ (lower than −15‰) in the

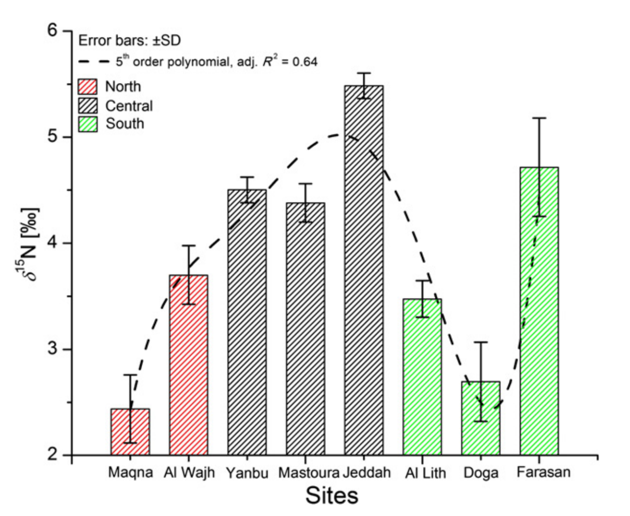

Fig. 4. Spatial variations in mean (±SD) particulate organic matter (POM) $\delta^{15}N$ values in the northern, central and southern Red Sea. The overlaid 'best fit' 5th order polynomial interpolation aids visualizing the spatial variation ($y = -3.45 + 10.38x + -6.03x^2 + 1.75x^3 + -0.24x^4 + 0.01x^5$).

Table 3
Linear regression coefficients of environmental variables, $\delta^{13}C$ and $\delta^{15}N$ values, and relative trophic position (RTP).

Variables		Coefficients				
Dependent	Independent	Nonstandardized		Standardized		
		β	SE	β	T	p
$\delta^{15}N$	Constant	406.093	145.221		2.796	*
	Chlorophyll *a*	0.0001	0.001	0.076	0.328	n.s.
	PSU	−10.800	3.703	−3.532	−2.917	*
	Temperature	−0.207	0.363	−0.125	−0.571	n.s.
	TN	−9.994	2.325	−2.394	−4.299	***
	Silicate	25.264	6.788	2.387	3.722	***
	TN:TP	−0.080	0.066	−0.181	−1.225	n.s.
	TN:Si	2.767	0.661	2.057	4.183	***
	Latitude	1.629	0.612	2.325	2.661	*
$\delta^{13}C$	Constant	−793.388	200.242		−3.962	***
	Chlorophyll *a*	−0.002	0.001	−0.735	−2.642	*
	PSU	19.804	5.106	5.651	3.887	**
	Temperature	1.728	0.501	0.909	3.453	**
	TN	6.847	3.206	1.430	2.136	*
	Silicate	0.644	9.360	0.053	0.069	n.s.
	TN:TP	−0.234	0.091	−0.459	−2.584	*
	TN:Si	−0.756	0.912	−0.490	−0.829	n.s.
	Latitude	−3.299	0.844	−4.110	−3.909	***
RTP	Constant	229.246	47.587		4.817	***
	Chlorophyll *a*	0.001	0.001	1.173	4.712	***
	PSU	−6.069	1.213	−6.519	−5.002	***
	Temperature	−0.252	0.119	−0.498	−2.117	*
	TN	−2.321	0.762	−1.824	−3.046	*
	Silicate	0.545	2.224	0.169	0.245	n.s.
	TN:TP	−0.011	0.022	−0.083	−0.520	n.s.
	TN:Si	0.324	0.217	0.792	1.497	n.s.
	Latitude	1.186	0.201	5.559	5.911	***

n.s. = not significant.
*** $p \leq 0.0001$.
** $p < 0.001$.
* $p < 0.05$.

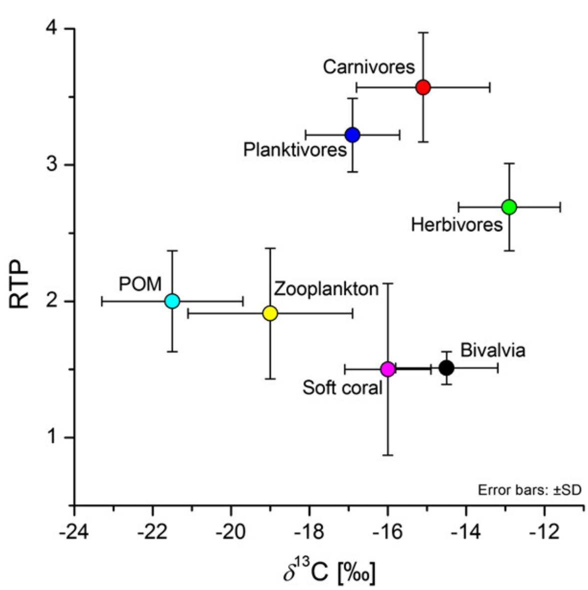

Fig. 5. Biplot of the study-wide mean (±SD) $\delta^{13}C$ values and relative trophic positions (RTPs) of particulate organic matter (POM) and coral reef biota in the Red Sea. Adductor muscle tissue of *T. squamosa* was used to infer a $\delta^{15}N$ baseline (Post, 2002) as a mixture of the isotopic values of N sources animals were exposed to over a relatively long period of time. N sources for *T. squamosa* include dissolved N (i.e. NH_4^+) utilized by its symbionts (autotrophy) and feeding on small-sized phytoplankton (heterotrophy). The trophic position of *Tridacna squamosa* (Bivalvia) was set to 1.5 to account for its mixotrophy. The trophic position of biota are expressed relative to *T. squamosa*.

northern region also exhibited lower RTPs, whereas at the Farasan archipelago animals with depleted $\delta^{13}C$ tended to attain higher RTPs (Fig. 7). Off Jeddah, relatively enriched $\delta^{15}N$ values were observed in POM (Fig. 4), and baseline-corrected RTPs of biota followed this trend. Ecohydrographic imprinting is most apparent in POM and zooplankton RTPs (Fig. 8), as these sample matrices reflect relatively short isotopic integration periods.

3.4. Dietary source contributions

The isotopic mixing model SIAR calculated food source contributions for each fish guild shown as modes, and lower and upper 95% credibility intervals (Fig. 9). The diet of the carnivorous *Cephalopholis hemistiktos* was isotopically based mainly on macronutrients originating from the reef. SIAR revealed a trend of increasing reliance of *C. hemistiktos* on reef-based resources from North to South (35–68%), but also pelagic macronutrients were a considerable dietary end member, as the SIAR model estimated a 30–38% contribution from zooplankton (Fig. 9). Particulate organic matter (POM) was a negligible isotopic end member for carnivores but in the North. Similarly, SIAR revealed that POM-derived macronutrients did not contribute considerably to the diet of *Acanthurus sohal* and *Ctenochaetus striatus* (herbivores). Reef-derived sources contributed 41–79% to the diet of herbivorous fishes, while the lowest contribution was determined for the central region where isotopically zooplankton-derived macronutrients accounted for 54% of the herbivores' diet. The importance of POM as isotopic end member tended to decrease from North to South for *Abudefduf sexfasciatus* (planktivores), and the model indicated that 82% of *A. sexfasciatus* elemental composition was explainable by feeding on zooplankton in the South (Fig. 9).

4. Discussion

This study is the first account of environmental controls and resource partitioning of consumers between pelagic and coral reef-derived macronutrients (C and N) over an unprecedented large spatial scale in the Saudi Arabian Red Sea. At first, the environmental setting is described. Although the Red Sea is generally considered as an oligotrophic ecosystem with low nutrient concentrations and primary production, environmental variables exhibit noteworthy variation at a latitudinal scale. Second, the strengths and weaknesses of C and N SIA for the collected biota in relation to their temporal integration of dietary signals are discussed. Thirdly, we discuss the C and N isotope ratios of coral reef biota with respect to the latitudinal gradient featured by the Red Sea and the potential resource utilization. It is suggested that urban eutrophication in the industrialized central region can be recognized in an isotopic offset to the natural latitudinal gradient from North to South, and that urban run-off alters the trophodynamics of consumers in coral reefs of the Saudi Arabian Red Sea.

4.1. Environmental variables

The nutrient sources to the Red Sea include the intrusion of Indian Ocean water, deep-water mixing, aerosol deposition, atmospheric N_2 fixation by algae, and urban run-off (Aberle et al., 2010; Acker et al., 2008; Raitsos et al., 2013; Sofianos and Johns, 2007; Wankel et al., 2010). The only available long-term biological dataset at large spatial and temporal scales are remotely-sensed observations of chlorophyll from satellite measurements of ocean color (Brewin et al., 2013). Off shore, hydrographic gradients of salinity, temperature and chl *a* have been used as identifiers for the origin and transformation of Red Sea water masses (Neumann and McGill, 1962; Patzert, 1974; Raitsos et al., 2013; Sofianos and Johns, 2007). Using chl *a* as a proxy for phytoplankton biomass and trophic status of the environment (Håkanson et al., 2007), the sites Maqna and Al Wajh are representative of the very oligotrophic northern Red Sea, whereas the site at the Farasan

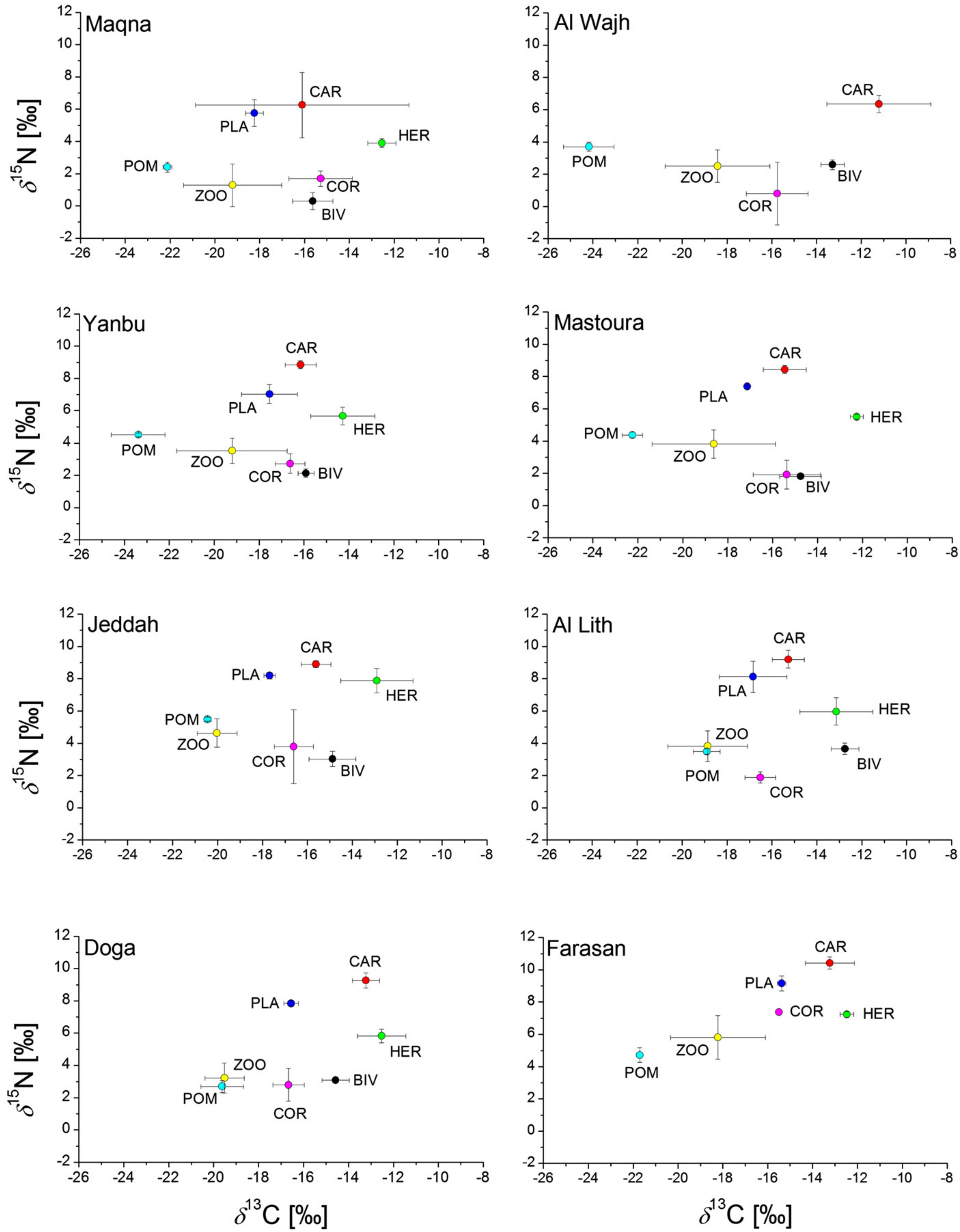

Fig. 6. Biplots of δ^{13}C and δ^{15}N values. δ^{13}C and δ^{15}N values (mean ± SE) of particulate organic matter (POM) and coral reef biota aggregated to ecological guilds at (a) Maqna in the Gulf of Aqaba, (b) Al Wajh, (c) Yanbu, (d) Mastoura, (e) Jeddah, (f) Al Lith, (g) Doga and (h) the Farasan archipelago following the latitudinal gradient from North to South.

Table 4
Two-way-ANOVA testing the null hypotheses that means of relative trophic positions (RTP) and $\delta^{13}C$ values are not significantly different between regions, guilds and for the interaction term between both nominal variables.

Source of variation	*df*	RTP		$\delta^{13}C$	
		MS	*F*	MS	*F*
Region (***)	2	1.397	8.886	44.170	14.526
Guild (***)	6	43.059	273.949	557.394	183.312
Region × Guild (***)	12	0.566	3.598	13.476	4.432
Error	683	0.157			
Total	704				

*** $p \leq 0.0001$.

archipelago in the South can be classified as mesotrophic (Fig. 2c). Chl *a* concentrations shown in the present study do not greatly depart from previous observation in the coral reefs in the Gulf of Aqaba and the open Red Sea (Acker et al., 2008; Al-Najjar et al., 2007; Genin et al., 2009; Raitsos et al., 2013). The reduced salinity, higher temperature and larger phytoplankton biomass (Table 1, Fig. 2) characterize the site at the Farasan archipelago and corroborate that nutrient rich, less saline Indian Ocean water intrusions influence the environmental conditions in the South (Raitsos et al., 2013). The very oligotrophic northern domain and the mesotrophic southern region therefore constitute two oceanographic end members along the stretch of the Red Sea. Salinity, temperature TN:TP and chl *a* are identified as important principal components that separate the sampling sites into three regions based on isotope data (Fig. 3). Phytoplankton biomass was inversely correlated with TN:TP. This relationship corroborates the conceptual understanding that TN:TP ratios above the Redfield ratio (TN:TP > 16–22) are typical for oligotrophic ecosystems, indicate phosphorous limitation rather than limitation by N or other nutrients, however, advance the development of N fixation processes due to the generally low fixed-N concentration (Deutsch et al., 2007; Downing, 1997; Geider and La Roche, 2002; Guildford and Hecky, 2000; Karl et al., 2002). The positive correlation of chl *a* with silicate availability and its stoichiometric derivatives TP:Si and TN:Si (Fig. 3) suggests that silicate availability significantly

Table 5
Pairwise comparisons of relative trophic positions (RTPs) and $\delta^{13}C$ for guilds across Red Sea regions (N = North, C = Central, S = South), and indicating the mean (±SD) difference for each guild from region to region.

Guild	Region	RTP			$\delta^{13}C$		
		Mean difference	SD	*p*	Mean difference [‰]	SD	*p*
Bivalves	N × C	0.77	0.5	n.s.	0.77	0.5	n.s.
	N × S	0.01	0.1	n.s.	−0.91	0.5	n.s.
	C × S	0.01	0.1	n.s.	−1.67	0.5	**
Soft coral	N × C	−0.40	0.2	n.s.	0.52	0.9	n.s.
	N × S	−0.27	0.2	n.s.	0.78	1.1	n.s.
	C × S	0.13	0.2	n.s.	0.25	1.0	n.s.
Zooplankton	N × C	−0.40	0.1	***	0.40	0.2	n.s.
	N × S	−0.29	0.1	***	−0.07	0.2	n.s.
	C × S	0.11	0.1	*	−0.47	0.2	*
Herbivores	N × C	−0.17	0.1	n.s.	0.60	0.6	n.s.
	N × S	0.15	0.1	n.s.	0.16	0.6	n.s.
	C × S	0.32	0.1	**	−0.44	0.5	n.s.
Planktivores	N × C	0.14	0.2	n.s.	−0.67	0.9	n.s.
	N × S	0.13	0.2	n.s.	−2.01	0.8	*
	C × S	−0.01	0.1	n.s.	−1.33	0.5	**
Carnivores	N × C	−0.48	0.1	***	−1.38	0.5	**
	N × S	−0.54	0.1	***	−3.33	0.5	***
	C × S	−0.06	0.1	n.s.	−1.95	0.4	***
POM	N × C	−0.30	0.2	n.s.	−1.13	0.9	n.s.
	N × S	0.29	0.2	n.s.	−2.96	0.9	***
	C × S	0.59	0.2	***	−1.83	0.8	*

n.s. = not significant.
* $p \leq 0.05$.
** $p < 0.001$.
*** $p < 0.0001$.

Table 6
Mean (±SD) relative trophic position (RTP), $\delta^{13}C$, and $\delta^{15}N$ values of biota in the northern, central and southern Red Sea (n = number of samples).

Factor	Guild	Region								
		North			Central			South		
		Mean	SD	n	Mean	SD	n	Mean	SD	n
RTP	Bivalve	1.5	0.14	22	1.5	0.12	22	1.5	0.10	20
	Soft coral	1.3	0.78	6	1.7	0.35	10	1.5	0.88	5
	Zooplankton	1.7	0.43	101	2.1	0.30	133	2.0	0.58	144
	Herbivores	2.7	0.09	10	2.9	0.27	30	2.5	0.34	30
	Planktivores	3.3	0.26	5	3.2	0.16	22	3.2	0.33	29
	Carnivores	3.2	0.57	18	3.6	0.15	30	3.7	0.31	40
	POM	2.0	0.20	6	2.3	0.05	9	1.7	0.38	12
$\delta^{13}C$	Bivalve	−14.6	1.4	22	−15.3	0.9	22	−13.7	1.1	20
	Soft coral	−15.6	1.3	6	−16.1	1.2	10	−16.4	0.7	5
	Zooplankton	−18.8	2.3	101	−19.2	2.3	133	−18.8	1.8	144
	Herbivores	−12.5	0.6	10	−13.1	1.5	30	−12.7	1.1	30
	Planktivores	−18.2	0.4	5	−17.6	0.8	22	−16.2	1.1	29
	Carnivores	−17.1	0.8	18	−15.7	0.8	30	−13.8	1.3	40
	POM	−23.1	1.3	6	−22.0	1.4	9	−20.2	1.3	12
$\delta^{15}N$	Bivalve	1.3	1.2	22	2.5	0.6	22	3.4	0.4	20
	Soft coral	1.1	1.6	6	2.6	1.2	10	3.3	2.4	5
	Zooplankton	1.8	1.3	101	3.9	1.0	133	4.6	1.6	144
	Herbivores	3.9	0.3	10	6.4	1.2	30	6.3	0.8	30
	Planktivores	5.8	0.8	5	7.6	0.7	22	8.4	0.8	29
	Carnivores	6.7	0.8	18	8.7	0.3	30	9.8	0.7	40
	POM	3.1	0.7	6	4.8	0.5	9	3.9	1.0	12

enhances the phytoplankton production in the coastal Red Sea. Higher phytoplankton biomass and TN concentrations at Al Lith, which demarks the northern extent of the Farasan Banks, were possibly related to the effluents of a large aquaculture facility. It is suggested that its discharge may affect the development of phytoplankton (Mohamed and Al-Shehri, 2012). In fact, phytoplankton at Al Lith was dominated by the filamentous *Trichodesmium erythraeum* (Cyanobacteria) and diatoms during the sampling period in October 2011 (pers. observation from microscopic cell counts). Decreased silicate concentrations at Al Lith may be attributed to the requirement of diatoms for silicate and explain silicate depletion (low Si:N) relative to the other sites (Table 1). The nutrient inventory and primary production of the Farasan Banks region may be of particular importance in winter, when climatological conditions export near shore water toward the open sea (Raitsos et al., 2013). Thus, from the nutrient source perspective the Red Sea can be regarded as a complex system, while each nutrient, i.e. N, source carries characteristic isotope signatures shaping the Red Sea isoscape (see Section 4.5. *Red Sea isoscape*).

4.2. Temporal scale-dependent constraints of isotope values

When interpreting the results of this study it must be acknowledged that the presented $\delta^{13}C$ and $\delta^{15}N$ values from Red Sea coral reefs convey biota-specific information integrated at different temporal scales. C and N SIA generally provides superior information on trophodynamics by integration of dietary patterns (isotopic end members) over longer periods of time as compared to snapshot information generated by gut content analysis (Pinnegar and Polunin, 2000). The integration period of consumers generally relates to ontogenetic and temperature-dependent characteristics of each species, including growth, life span, and/or developmental stage duration. Elemental turnover rates in fish muscle and isotopic equilibration with diet, for instance, ranges from several months to years (Herzka, 2005; Hesslein et al., 1993; Pinnegar and Polunin, 1999; Sweeting et al., 2005). Tending toward 4–6 months through years, the equilibration periods of slow-growing filter-feeding Bivalvia are relatively long as well (Cabana and Rasmussen, 1996; Fukumori et al., 2008; Jennings and Warr, 2003; Raikov and Hamilton, 2001). We therefore assume that macrofauna $\delta^{13}C$ and $\delta^{15}N$ values of the present study reflect the isotopic composition of their diet over several months and average out short term seasonal variation. Conversely,

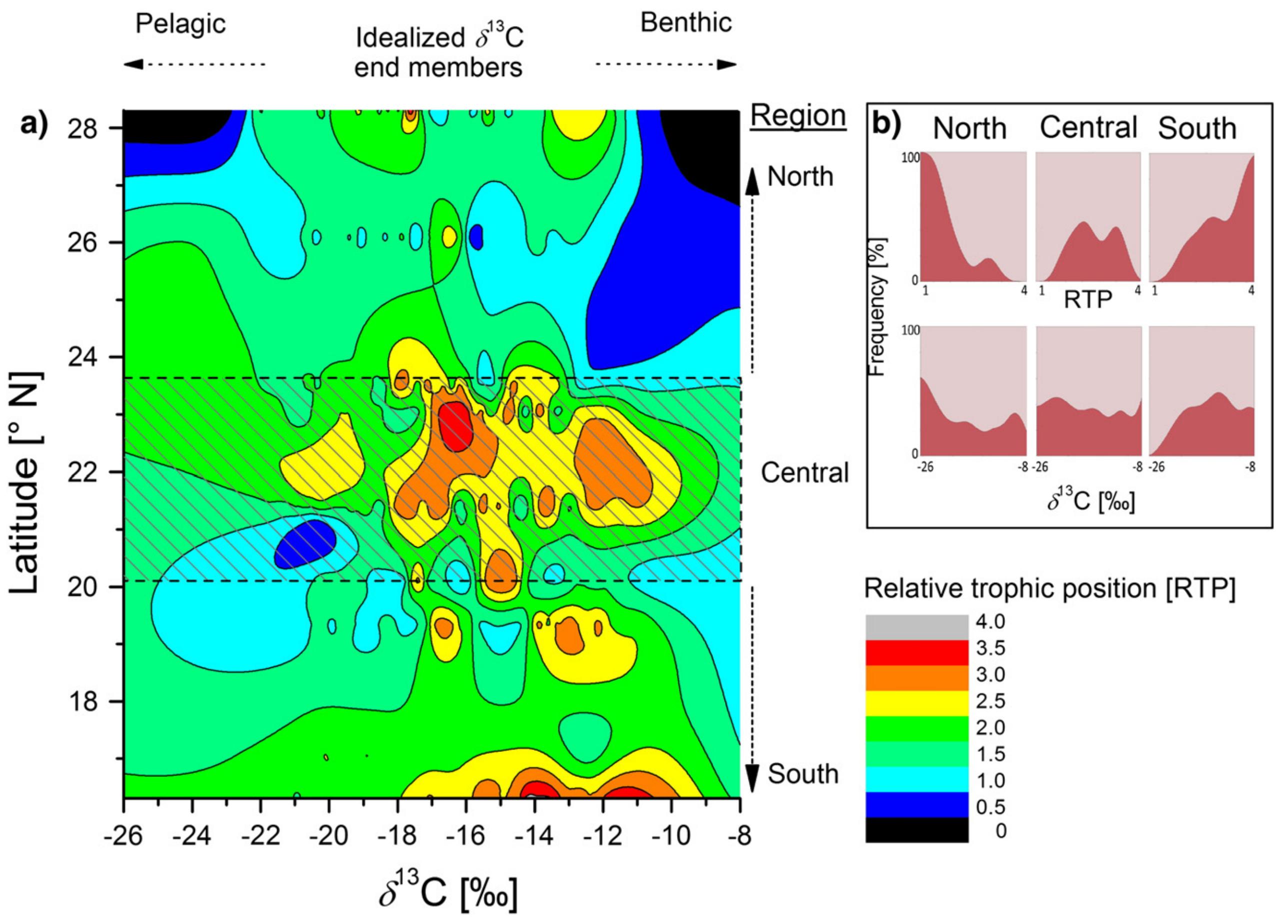

Fig. 7. Ecohydrographic pattern in isotopic composition. Two-dimensional contour plot (a) of latitude [°N], δ^{13}C signatures [‰] and relative trophic position (RTPs, color coding) of samples collected in the Red Sea during the expedition in September and October 2011, and (b) frequency distribution (% of cases) of RTP and δ^{13}C values in three Red Sea regions (North, Central, South). Dotted arrows above Fig. 7a indicate tendency of δ^{13}C values toward pelagic (depleted) and benthic coral reef (enriched) end members (Marshall et al., 2007; Muscatine et al., 1989).

the isotopic values of POM reflect the shortest temporal snapshot of dietary end members in this study and with only one sampling instance at each site data cannot account for fluctuations in δ^{13}C and δ^{15}N values attributable to seasonal changes of phytoplankton growth (Burkhardt et al., 1999b; Kürten et al., 2011; Mariotti et al., 1984; Rau et al., 1996). Overlapping size ranges of bacteria, phytoplankton, zooplankton, and non-living components contained in POM generally complicate

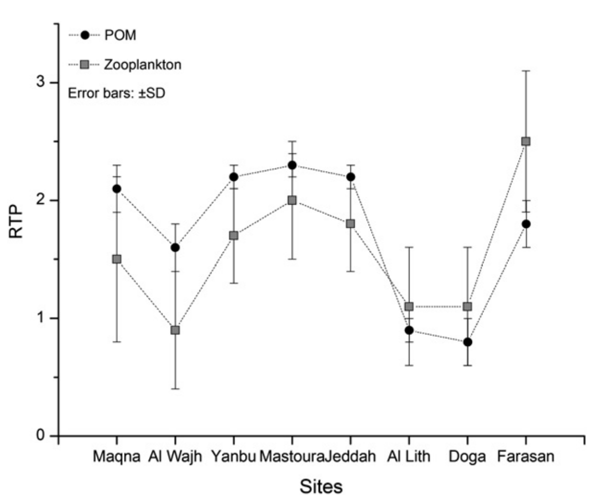

Fig. 8. Spatial correlation of mean (±SD) particulate organic matter (POM) and zooplankton relative trophic positions (RTPs) in the Red Sea.

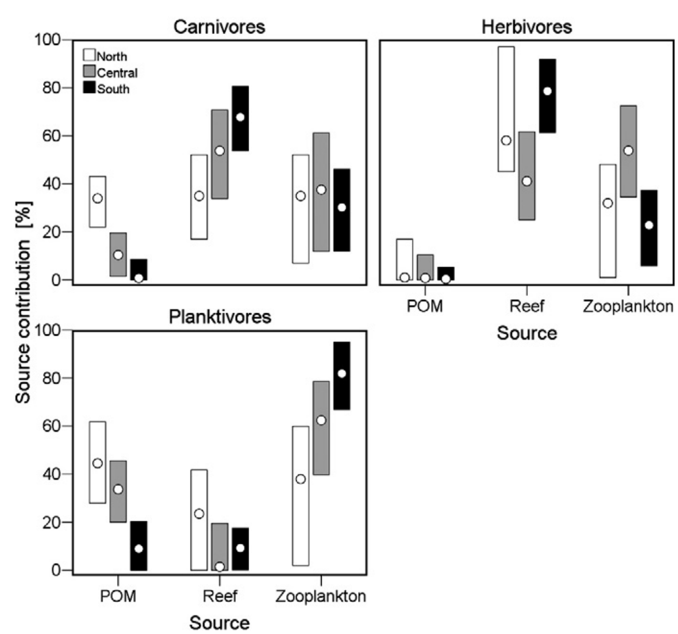

Fig. 9. Contributions (%) of potential coral reef-derived and pelagic (POM, zooplankton) macronutrient end members as determined by the Bayesian mixing model SIAR (POM) shown as 95% credibility intervals (boxes) and respective Bayesian distribution modes (circles) to the isotopic composition of carnivorous, herbivorous, and planktivorous fishes during the sampling period in September–October 2011 at coral reefs in the northern, central and southern Red Sea.

their physical separation prior to SIA which reduces the value of POM as isotopic baseline (Hamilton et al., 2005; Harmelin-Vivien et al., 2008). Thus, despite screening through a 50 μm mesh, POM samples may not adequately reflect the isotopic baseline values obligate photoautotrophs exhibit and may explain the higher baseline-corrected RTPs measured for POM in relation to zooplankton at most study sites (Fig. 8). Somewhat longer isotopic integration periods of dietary end members are expected for zooplankton that temporally lags behind the short-term isotopic variability of primary producers. The isotopic composition of its prey typically manifests in zooplankton δ^{13}C and δ^{15}N values typically in one to three weeks (c.f. Bonnet et al., 2005; Halsband-Lenk et al., 2002), though copepodite stage-duration in subtropical seas is relatively short, i.e. <1–2 days for *Acrocalanus gibber* (Copepoda; McKinnon, 1996). Thus, having collected the same biota at each site, differences in isotope values and RTPs reflect the variation in trophodynamics and isotopic end members at ecohydrographic (latitudinal) scale from the oligotrophic Gulf of Aqaba toward the mesotrophic Farasan archipelago at variable temporal resolution (Post, 2002).

4.3. Isotopic values of invertebrates

Zooplankton comprised a range of taxa with overlapping trophic roles including true herbivores such as Pteropoda and Ostracoda, predatory zooplankton such as Chaetognatha, and omnivorous Copepoda. Calanoid Copepoda constituted the most diverse and abundant taxonomic group followed by Cyclopoida and Poecilostomatoida (Kürten et al., unpub. data). The zooplankton guild exhibited the largest range of δ^{13}C and δ^{15}N values in this study and mirrors the variety of ecological niches occupied by functionally different zooplankton groups. At the latitudinal scale mean (±SD) zooplankton δ^{15}N values increased from North (1.8 ± 1.3‰) to South (4.6 ± 1.6‰) (Table 6) which reflects the relative larger importance of atmospheric vs. deep-water nitrates as N source in the North (see discussion below). The most depleted zooplankton group was formed by zoeae (Decapoda) with a δ^{15}N of −1.5‰ at Maqna, whereas the most ^{15}N enriched species was the predatory copepod *Euchaeta* sp. (8.9‰) at Farasan. There are few studies to compare the SIA data of Red Sea zooplankton at the species level to. The range of zooplankton δ^{15}N values of the present study, however, is similar to δ^{15}N values of zooplankton in the Gulf of Aqaba, where low δ^{15}N values of zooplankton were attributed to 'new N' from atmospheric origin as opposed to N fixed by *Trichodesmium* spp. and upwelled nitrate (Aberle et al., 2010).

Tridacna squamosa (Cardiidae) and soft corals of the genera *Sinularia* and *Sarcophyton* (Alcyonidae) showed δ^{15}N values below or close to 0‰, which is in general indicative for the utilization of N from atmospheric origin and its diazotrophic N_2 fixation (Alamaru et al., 2009; Lesser et al., 2007; Minagawa and Wada, 1984; Montoya et al., 2002; Wankel et al., 2010). In fact, a few specimens of *T. squamosa* collected at Maqna and Al Wajh exhibited δ^{15}N values of −1.4 to 0.2‰. This is a realistic result, because *T. squamosa*, *Sinularia* sp. and *Sarcophyton* sp. on the one hand host symbiotic zooxanthellae, but on the other hand rely for their growth on feeding on phytoplankton and suspended particles (Fabricius and Klumpp, 1995; Jantzen et al., 2008; Khalesi et al., 2011). The δ^{15}N values of *T. squamosa* therefore reflect a conservative estimate of the isotopic baseline as a mixture of a range of basal biotic and abiotic N sources. Alcyonidae may constitute an important trophodynamic vector for macronutrients from the pelagic to the benthic domain and toward its predators by feeding on phytoplankton and suspended matter and subsequent accumulation and conversion to essential polyunsaturated fatty acids (PUFAs) including EPA (20:5n−3) and DHA (22:6n−3) in their tissues (Fabricius and Dommisse, 2000; Khalesi et al., 2011). According to their ^{13}C enrichment relative to each other, soft corals were mostly ^{13}C depleted compared to *T. squamosa* (Figs. 3, 4). The relative positioning in isotope biplots therefore suggests a higher importance of autotrophy vs. heterotrophy for *T. squamosa* as compared to Alcyonidae. Achituv et al. (1997) drew a similar conclusion regarding oceanic vs. reef-derived end members for barnacles in coral reefs in the Gulf of Aqaba, because typical oceanic resources usually attain δ^{13}C values of −21‰ whereas δ^{13}C values of primary producers in coral reefs tend toward −14 to −10‰ (Kolasinski et al., 2011; Muscatine et al., 1989). As barnacle δ^{13}C were −17 to −19.7‰, significant resourcing from producers within the reef (−11‰) was proposed (Achituv et al., 1997). Usually, allochthonous macronutrients sources are important to coral reef biota (Genin et al., 2009; Wyatt et al., 2010a, 2013; Yahel et al., 1998), but the positioning in isotope space in the present study suggests that neither POM nor zooplankton contribute isotopically to the diet of soft corals and *T. squamosa* (Fig. 5). We note that the isotopic inventory of POM and zooplankton during our expedition period may depart from long-term integrated information that can be deduced from e.g. *T. squamosa*. In addition, our different observation may be related to the fact that POM comprised also living and non-living particles (particle size 0.7–50 μm, this study), and that isotopes from various other sources mask the isotope ratio of the true potential dietary end members for soft coral and *T. squamosa*.

4.4. Isotopic values of fishes

The carnivorous grouper *Cephalopholis hemistiktos* (Serranidae) is the most abundant member of the genus *Cephalopholis* throughout the Red Sea (Randall and Ben-Tuvia, 1983). In the present study, *C. hemistiktos* exhibit the most ^{15}N enriched isotope ratios compared to the other biota (Figs. 5, 6), but exhibit on average only small δ^{15}N enrichment relative to *A. sexfasciatus*; at Maqna δ^{15}N and δ^{13}C even overlapped. *C. hemistiktos* occurs predominantly from the shallow reef-top to 30 m depths and preys mainly on benthic crustaceans as well as pomacentrid and gobiid fish (Shpigel and Fishelson, 1989a,b). The estimated RTP for *C. hemistiktos* reported in the present study (3.68 ± 0.3, mean ± SD) concurs with estimates from dietary studies (RTP = 4.1 ± 0.7; Froese and Pauly, 2013; Shpigel and Fishelson, 1989a,b). The SIAR model indicated an increasing contribution of reef-derived macronutrients to the diet of *C. hemistiktos* from North to South (Fig. 9). Zooplankton-derived macronutrients accounted for approximately 1/3 to its diet across all regions, while the importance of POM-derived macronutrients waned (Fig. 9). The isotopic source attribution to zooplankton and POM may relate to the predation on zooplanktivorous pomacentrid fishes by *C. hemistiktos*. Indeed, while carnivore RTPs increase significantly from North to South there is a significant enrichment in δ^{13}C values from −17.1 ± 0.8‰ to −13.8 ± 1.3‰, respectively (Tables 5, 6), which corroborates the indication of a larger contribution of reef-derived nutrition to the diet of *C. hemistiktos* by the SIAR model (Fig. 9). The reasons for this observation can only be speculated on. We suggest that both allochthonous and autochthonous macronutrient sources are of similar importance in the very oligotrophic North, where reefs with steep slopes and little deposition of organic material that supports benthic detrital food webs occur. In contrast the shallower shelf and flat reefs of the southern Red Sea, together with higher primary production and concomitantly larger deposition of organic material may support the benthic food web and increase the contribution of reef-derived macronutrients to the diet of *C. hemistiktos*.

Surgeonfish are known as reef sweepers and feeders on filamentous and surface film algae but only few surgeonfish species can be considered as true herbivores, because some species consume also reef-derived (detrital) material (Choat et al., 2004; Krone et al., 2011; Marshell and Mumby, 2012; Polunin et al., 1995). Herbivorous fishes in the present study included two species of surgeonfish (Acanthuridae), namely *Acanthurus sohal* and *Ctenochaetus striatus*, which both are highly abundant in Red Sea coral reefs (Bouchon-Navaro and Harmelin-Vivien, 1981). The potential diet of surgeonfish include macrophytes, turf algae, and calcareous Rhodophyta that can be as ^{13}C enriched as −4‰ (Carassou et al., 2008; Fry et al., 1982;

Yamamuro et al., 1995). POM was isotopically of negligible importance in the diet of surgeonfish (Fig. 9). In general, herbivorous fishes were enriched in ^{15}N relative to POM, zooplankton and soft corals (Fig. 6), and are significantly ^{13}C depleted in the southern Red Sea compared to animals collected in the North and Central region (Table 5). The SIAR model revealed that C and N sources for surgeonfish were mainly of reef-derived origin, but oceanic resources were also indicated (Fig. 9). The ^{13}C enrichment (~−12.5‰) but intermediate δ^{15}N (~5.7‰) of herbivores relative to *T. squamosa* and soft coral, corroborated that herbivores relied largely on reef-derived nutrition rather than pelagic end members, but zooplankton-derived macronutrients were important in the central Red Sea (Fig. 9). The RTPs of *Ctenochaetus striatus* (RTP = 2.76 ± 0.3) in the present study are marginally higher than the RTPs reported from reefs at the coast of Oman (RTP = 2; Mill, 2007) and New Caledonia (RTP = 1.5–2.0) for *C. striatus* (Carassou et al., 2008), and closer to the estimated RTP of *Acanthurus sohal* (RTP = 2.25 ± 0.3, this study). Surgeonfish occupied a somewhat higher RTP in the South (Table 5). This difference cannot be attributed to ontogenetic differences, because surgeonfish tend not to change their resource end members very much compared to carnivores that eat bigger prey as larger they become (Cocheret de la Morinière et al., 2003). It is recognized that differences in RTPs may relate to the fact that RTPs were calculated using Bivalvia δ^{15}N values, while algae that constitute the true food source were not sampled, however, we argue that seasonal variability in δ^{15}N values related to the growth of macroalgae are outweighed when using *T. squamosa* to infer RTPs.

The planktivorous damselfish *Abudefduf sexfasciatus* (Pomacentridae) feeds on zooplankton such as Chaetognatha, large Copepoda and other pelagic mesozooplankton during daylight hours and should be regarded as a representative of trophic level three (Fishelson, 1970; Frédérich et al., 2009). Feeding on mesozooplankton and resting in aggregated groups at night, *A. sexfasciatus* may import organic matter via its feces from the pelagic to the benthos and which may constitute an important conduit of macronutrients to coral reefs. In the present study, *A. sexfasciatus* occupied a RTP of 3.2 ± 0.3. Similarly, Mill (2007) reported a RTP of 3, however, these estimates are ~0.5 trophic levels higher than RTPs presented by Carassou et al. (2008; RTP = 2.2–2.5) and in FishBase (Froese and Pauly, 2013; RTP = 2.37). The difference of 2.8‰ for δ^{15}N and 1‰ for δ^{13}C (means of all sites) between zooplankton and *A. sexfasciatus*, respectively, tends toward the mean diet-tissue fractionation factor from previous meta-analyses (Post, 2002). However, the δ^{15}N TEF observed for *A. sexfasciatus* in the present study was marginally lower than the 3.2‰ $\Delta\delta^{15}$N between gut and tissues of *A. sexfasciatus* at Ningaloo Reef, Australia (Wyatt et al., 2010b). Wyatt et al. (2012b) documented more depleted δ^{13}C values in the tissues of planktivorous fish with decreasing distance to the ocean and interpreted this trend as increased reliance on oceanic productivity. Here, SIAR indicated the largest contribution of zooplankton to the diet of *A. sexfasciatus* in the South, whereas in the North and Central region POM-derived macronutrients appear to be of larger importance (Fig. 8). The reason for the relatively larger isotopic contribution of POM-derived (phytoplankton, detritus) C and N to the diet of *A. sexfasciatus* in the North may also relate to the trophic status of the system. The scarcity of phytoplankton (proxy chl *a*) and low zooplankton biomass (Kürten et al., unpub. data) may force *A. sexfasciatus* to include a higher degree of POM in its diet, while it can feed mainly on zooplankton alone in the South, where phytoplankton and zooplankton biomass is much larger. In fact, the relative positioning of biota in isotope space at Farasan compared to the other sites suggests a higher importance of allochthonous unidirectional macronutrient fluxes from POM to higher trophic levels (Fig. 6).

4.5. Red Sea isoscape

The present study revealed a spatial variation of δ^{13}C, δ^{15}N and RTP values pointing to a separation of the study sites into three ecohydrographic regions (Figs. 4, 7) concurrent with the broad meridional domains as indicated by satellite imagery (Raitsos et al., 2013). The relationships between ecohydrography and isotopic end members of the presented isoscape are discussed for δ^{15}N, followed by constraints by δ^{13}C and RTP values.

4.5.1. Explanation for the patterns in δ^{15}N

Nutrient concentrations and phytoplankton biomass increased markedly from the Gulf of Aqaba toward the Farasan Islands at the same time as the δ^{15}N of biota increased (Fig. 2, Table 6). This may relate to different principal N end members in each ecohydrographic region. We suggest that the correspondence of coral reef biota and POM isotope ratios with environmental factors and latitude display an ecohydrographic pattern with Maqna in the North and Farasan in the South as natural hydrographic end members within the Red Sea isoscape (Fig. 7). This overall trend concurs with early studies describing regional patterns of primary production and hydrography that were initially related mainly to the changes in wind direction (e.g. Edwards, 1987; Halim, 1984; Neumann and McGill, 1962 and references therein; Patzert, 1974). However, more recent studies showed that the Red Sea ecosystem is by far more complex as to its hydrodynamics and nutrient (N) sources fuelling primary production (Raitsos et al., 2013). By means of remote sensing datasets, both Acker et al. (2008) and Raitsos et al. (2013) noted in addition increased fluorescence along the Red Sea coast and highlighted that (off shore) primary production was sustained by coral reefs and archipelagos in the coastal Red Sea.

As mentioned above, N sources in the Red Sea include the intrusion of Indian Ocean water, deep-water mixing, aerosol deposition, atmospheric N_2 fixation by algae, and urban run-off (Aberle et al., 2010; Acker et al., 2008; Raitsos et al., 2013; Sofianos and Johns, 2007; Wankel et al., 2010). Carrying distinctive δ^{15}N values, SIA potentially allows discriminating between N end members. In most oceanic environments nitrate supply from below the euphotic zone is the primary source of N for primary producers (Graham et al., 2010). The δ^{15}N of nitrate (NO_3^-) in the ocean subsurface has been considered as a relatively sensitive indicator of ocean system processes both denitrification and N fixation (Deutsch et al., 2007; Sigman et al., 2000). Typically, subsurface NO_3^- attains δ^{15}N values of ~5‰ relative to atmospheric N_2 with a δ^{15}N of ~0‰ (Sigman et al., 2000). Other potential N subsidies include sewage with a typically enriched δ^{15}N value (Savage, 2005), and N from aerosol deposition which shows depleted δ^{15}N values of −3.4‰ in winter in the Gulf of Aqaba (Wankel et al., 2010).

The rapid and unprecedented industrial and urban development in the Kingdom of Saudi Arabia at Jeddah and Yanbu has resulted in frequent discharges of domestic and commercial wastewater to the coastal waters. Records of enriched δ^{15}N in coastal environments were frequently used as indicators of anthropogenic sources, including sewage, wastewater discharges, terrestrial run-off after precipitation, and agricultural fertilizers (e.g. Fertig et al., 2009; McClelland et al., 1997; Risk et al., 2009a; Savage, 2005; Vizzini and Mazzola, 2006). Here, isotopically enriched values of POM and zooplankton in the central Red Sea at Jeddah were documented (Fig. 3). This signal is interpreted as a result of the deteriorated water quality caused by urban discharges from Jeddah (Risk et al., 2009b; this study). In fact, sewage-derived ^{15}N enrichment signals were documented in corals as far as 15 km off shore of Jeddah and linked to the city's rapid expansion and concomitant population growth since the 1950s (Risk et al., 2009b). Thus, this study concurs with previous reports which suggested an anthropogenic fingerprint from urban run-off on isotope values of coral reef biota.

Conversely, at oligotrophic sites such as in the Gulf of Aqaba the importance of atmospheric N deposition and fixation of 'new N' as indicated by depleted δ^{15}N, may compensate the requirement of phytoplankton for N (Aberle et al., 2010; Chen et al., 2007; see discussion below). This is reflected for example in δ^{15}N < 0‰ of herbivorous zooplankton (Aberle et al., 2010), and in low mean (±SD) POM δ^{15}N values of 2.4 ± 0.3‰ at Maqna (Fig. 3). Similarly, Hauss et al. (2013)

distinguished the relative contribution of atmospheric vs. sub-surface N end members for zooplankton based on low δ^{15}N being indicative for N_2 fixation and higher δ^{15}N for oceanic N in the tropical Northern Atlantic. Our opinion is supported furthermore by recent studies which suggest a larger general importance of 'new N' from atmospheric deposition and diazotrophic N_2 fixation by picophytoplankton and *Trichodesmium erythraeum* (Cyanobacteria) in oligotrophic, subtropical ecosystems (McClelland et al., 2003; Montoya et al., 2002). This is also consistent with the observation of comparatively low δ^{15}N values of POM and zooplankton at Al Lith, where the N fixing *T. erythraeum* was present during the sample collection for this study (Kürten et al., unpub. data).

4.5.2. Explanation for the patterns in δ^{13}C

Marine biota exhibit a broad range of ^{13}C values, but differences in δ^{13}C potentially allow the discrimination between pelagic/oceanic vs. benthic resources in coral reefs (Kolasinski et al., 2011; Wyatt et al., 2012b). Phytoplankton as primary producers form dietary end members from the ocean catchment for consumers in coral reefs as opposed to benthic primary producers such as macroalgae (Lamb and Swart, 2008; Wyatt et al., 2010a, 2012b, 2013). Oceanic phytoplankton typically attains depleted δ^{13}C values (−18 to −22.2‰), although high δ^{13}C values of up to −28.8‰ can occur in Cyanophyceae, and Cryptophyceae can be ^{13}C enriched up to −5.5‰ (Falkowski, 1991). Several studies revealed taxon-specific variability and responses to environmental conditions that influence phytoplankton growth rates and therefore C isotopic fractionation (Burkhardt et al., 1999a,b; Falkowski, 1991; Fry and Wainwright, 1991). Benthic primary producers, in contrast, attain δ^{13}C values typically in the range of −11 to −5‰ (Gearing et al., 1984; Heikoop et al., 2000; Peterson and Fry, 1987; Yamamuro et al., 1995). Concurrent with this generalization the present study showed that reef-associated herbivorous fish, soft corals and bivalves were distinguished by depleted δ^{15}N and enriched δ^{13}C signatures from planktivores, carnivores and zooplankton (Fig. 6). Thus, irrespective of the taxonomic identity of biota, an approximation of dietary end members based on the δ^{13}C scale can be inferred (Fig. 7).

4.5.3. Explanation for the patterns in RTPs

Regardless of decreasing signal strength of basal variability toward higher trophic levels (Iverson, 2009), it has been shown that ecohydrography alters the isotopic values of both δ^{13}C and δ^{15}N at the base of marine food webs, and that spatial and/or seasonal variations thereof can propagate from primary producers toward zooplankton and other higher trophic level biota (Aberle et al., 2010; Hauss et al., 2013; Kürten et al., 2011, 2012). Here, δ^{13}C and δ^{15}N values suggested two principle N end members at the latitudinal (Maqna vs. Farasan) and at the cross-reef spatial scale (oceanic vs. reef). Anthropogenic activities in the central region of the Red Sea between 20 and 24° N were noticeable as an offset to the natural gradient toward higher biota δ^{15}N as well as toward higher baseline corrected RTPs (Table 6; Fig. 7). Because we detected this pattern also in the RTP data, we suggest that highly intertwined processes shape the Red Sea isoscape and coral reef trophodynamics. The separation into three ecohydrographic regions and δ^{15}N enrichment in the central region suggests that there is a change in δ^{15}N values that was most likely attributable to the urban run-off and that the variation in isotopic baseline signals propagates toward higher trophic levels. But, since at the same time we also documented higher RTPs for the same region, we suggest that the urban run-off also alters the trophodynamics. Sommer et al. (2002) hypothesized that cascading bottom–up processes potentially alter the configuration of food webs and that the length of the food chain from primary producers to higher trophic levels should depend on nutrient richness and stoichiometry. For oligotrophic ecosystems under the influence of urban eutrophication it was hypothesized that the heterotrophic microbial food web adds additional trophic links. Having evidence for urban eutrophication and increased RTPs, we consider this theoretically plausible.

5. Conclusions

The present study supports the notion that reefs depend on suspended particles and dissolved nutrients trapped from the flowing water, whereas the relative dependence on allochthonous macronutrient end members may vary substantially in time and space (Furnas et al., 2005; Monismith et al., 2006; Wyatt et al., 2010a, 2012a; Yahel et al., 1998). Isoscapes offer large potential to refine our understanding of biogeochemical cycles, constrain functional connectivity of seascapes, and to elucidate migration and dispersal of marine organisms' at large spatial scales (Bowen, 2010; Hobson, 1999; McMahon et al., 2013; Schell et al., 1998). Integrating isotopic end member signals at short and long temporal scales, this study reveals a robust geographical end-to-end pattern for POM through zooplankton and higher trophic levels including herbivorous, planktivorous and carnivorous fishes. If so, this argues for the interpretation that the recognized isotopic pattern of the Red Sea relates to the relative importance of N_2 fixation in the northern region vs. oceanic primary production in the southern Red Sea which is sustained by nutrients (N) from the Indian Ocean. Both, δ^{15}N values and RTPs tend to increase from North to South, but anthropogenic activities in the central region of the Red Sea between 20 and 24° N alter the relative importance of this N fixation pathway in the central Red Sea and were noticeable as an offset to this natural gradient regardless whether consumers derive their macronutrients from ^{13}C depleted oceanic end members or from ^{13}C enriched coral reef-derived sources. Although numerous intertwined processes influence the ecohydrography and biogeochemistry of the Red Sea, the presented isoscape highlights the complexity of coral reefs and the oceanic catchment for coral reefs along the Red Sea coast of Saudi Arabia.

Supplementary data to this article can be found online at http://dx.doi.org/10.1016/j.seares.2013.07.008.

Acknowledgements

This collaboration of the Jeddah Transect Project between King Abdulaziz University and Helmholtz-Center for Ocean Research GEOMAR was funded by the King Abdulaziz University (KAU) Jeddah, Kingdom of Saudi Arabia under grant No. T-065/430-DRS. The authors, therefore, acknowledge with thanks the KAU for technical and financial support. The authors thank the Royal Commission for Jubail and Yanbu, and National Prawn Company for accommodation, access to boats and research areas. We are thankful to S. Audritz, R. Devassy, T. Hansen, B. Huang, and M. El-Sherbini for assistance during sample collection, analytical and technical support. We thank the divers S. Al-Ahmadi, A. Gashgari and M. Qoqandi as well as all other participants in the expedition for their supportive actions. We also thank one anonymous reviewer for providing ample comments on earlier versions of this manuscript.

References

Aberle, D., Hansen, T., Boettger-Schnack, R., Burmeister, A., Post, A.F., Sommer, U., 2010. Differential routing of 'new' nitrogen toward higher trophic levels within the marine food web of the Gulf of Aqaba, Northern Red Sea. Marine Biology 157, 157–169.

Abu-Hilal, A., Al-Najjar, T., 2009. Marine litter in coral reef areas along the Jordan Gulf of Aqaba, Red Sea. Journal of Environmental Management 90, 1043–1049.

Achituv, Y., Brickner, I., Erez, J., 1997. Stable carbon isotope ratios in Red Sea barnacles (Cirripedia) as an indicator of their food source. Marine Biology 130, 243–247.

Acker, J., Leptoukh, G., Shen, S., Zhu, T., Kempler, S., 2008. Remotely-sensed chlorophyll *a* observations of the northern Red Sea indicate seasonal variability and influence of coastal reefs. Journal of Marine Research 69, 191–204.

Alamaru, A., Loya, Y., Brokovich, E., Yam, R., Shemesh, A., 2009. Carbon and nitrogen utilization in two species of Red Sea corals along a depth gradient: insights from stable isotope analysis of total organic material and lipids. Geochimica et Cosmochimica Acta 73, 5333–5342.

Al-Najjar, T., Badran, M.I., Richter, C., Meyerhoefer, M., Sommer, U., 2007. Seasonal dynamics of phytoplankton in the Gulf of Aqaba, Red Sea. Hydrobiologia 579, 69–83.

Bearhop, S., Adams, C.E., Waldron, S., Fuller, R., Macleod, H., 2004. Determining trophic niche width: a novel approach using stable isotope analysis. Journal of Animal Ecology 73, 1007–1012.

Bonnet, D., Richardson, A., Harris, R.P., Hirst, A., Beaugrand, G., Edwards, M., Ceballos, S., Diekman, R., López-Urrutia, A., Valdes, L., Carlotti, F., Molinero, J.C., Weikert, H., Greve, W., Lucic, D., Albaina, A., Yahia, N.D., Umani, S.F., Miranda, A., dos Santos, A., Cook, K., Robinson, S., Fernandes de Puelles, M.L., 2005. An overview of *Calanus helgolandicus* ecology in European waters. Progress in Oceanography 65, 1–53.

Bosley, K.L., Wainright, S.C., 1999. Effects of preservatives and acidification on the stable isotope ratios (^{15}N:^{14}N, ^{13}C:^{12}C) of two species of marine animals. Canadian Journal of Fisheries and Aquatic Sciences 56, 2181–2185.

Bouchon-Navaro, Y., Harmelin-Vivien, M.L., 1981. Quantitative distribution of herbivorous reef fishes in the Gulf of Aqaba (Red Sea). Marine Biology 63, 79–86.

Bowen, G., 2010. Isoscapes: spatial pattern in isotopic biogeochemistry. Annual Review of Earth and Planetary Sciences 38, 161–187.

Brewin, R.J.W., Raitsos, D.E., Pradhan, Y., Hoteit, I., 2013. Comparison of chlorophyll in the Red Sea derived from Modis-Aqua and in vivo fluorescence. Remote Sensing of Environment 136, 218–224.

Bunn, S.E., Loneragan, N.R., Kempster, M.A., 1995. Effects of acid washing on stable isotope ratios of C and N in penaeid shrimp and seagrass: implications for food-web studies using multiple stable isotopes. Limnology and Oceanography 40, 622–625.

Burkhardt, S., Riebesell, U., Zondervan, I., 1999a. Effects of growth rate, CO_2 concentration, and cell size on the stable carbon isotope fractionation in marine phytoplankton. Geochimica et Cosmochimica Acta 63, 3729–3741.

Burkhardt, S., Riebesell, U., Zondervan, I., 1999b. Stable carbon isotope fractionation by marine phytoplankton in response to daylength, growth rate, and CO_2 availability. Marine Ecology-Progress Series 184, 31–41.

Cabana, G., Rasmussen, J.B., 1996. Comparison of aquatic food chains using nitrogen isotopes. Proceedings of the National Academy of Sciences of the United States of America 93, 10844–10847.

Carabel, S., Godínez-Domínguez, E., Verísimo, P., Fernández, L., Freire, J., 2006. An assessment of sample processing methods for stable isotope analysis of marine food webs. Journal of Experimental Marine Biology and Ecology 336, 254–261.

Carassou, L., Kulbicki, M., Nicola, T.J.R., Polunin, N.V.C., 2008. Assessment of fish trophic status and relationships by stable isotope data in the coral reef lagoon of New Caledonia, southwest Pacific. Aquatic Living Resources 21, 1–12.

Chen, Y., Mills, S., Street, J., Golan, D., Post, A., Jacobson, M., Paytan, A., 2007. Estimates of atmospheric dry deposition and associated input of nutrients to Gulf of Aqaba seawater. Journal of Geophysical Research 112, 1–14.

Choat, J.H., Robbins, W.D., Clements, K.D., 2004. The trophic status of herbivorous fishes on coral reefs. Marine Biology 145, 445–454.

Cocheret de la Morinière, E., Pollux, B.J.A., Nagelkerken, I., Hemminga, M.A., Huiskes, A.H.L., van der Velde, G., 2003. Ontogenetic dietary changes of coral reef fishes in the mangrove-seagrass-reef continuum: stable isotopes and gut-content analysis. Marine Ecology-Progress Series 246, 279–289.

de Lecea, A.M., Cooper, R., Omarjee, A., Smit, A.J., 2011. The effects of preservation methods, dyes and acidification on the isotopic values ($\delta^{15}N$ and $\delta^{13}C$) of two zooplankton species from the KwaZulu-Natal Bight, South Africa. Rapid Communications in Mass Spectrometry 25, 1853–1861.

Deutsch, C., Sarmiento, J.L., Sigman, D.M., Gruber, N., Dunne, J.P., 2007. Spatial coupling of nitrogen inputs and losses in the ocean. Nature 445, 163–167.

Downing, J.A., 1997. Marine nitrogen:phosphorus stoichiometry and the global N:P cycle. Biogeochemistry 37, 237–252.

Edwards, F.J., 1987. Climate and oceanography. In: Edwards, A.J., Head, S.M. (Eds.), Key Environments—Red Sea. Pergamon Press, Oxford, pp. 45–69.

Fabricius, K.E., Dommisse, M., 2000. Depletion of suspended particulate matter over coastal reef communities dominated by zooxanthellate soft corals. Marine Ecology-Progress Series 196, 157–167.

Fabricius, K., Klumpp, D.W., 1995. Widespread mixotrophy in reef-inhabiting soft corals: the influence of depth, and colony expansion and contraction on photosynthesis. Marine Ecology-Progress Series 125, 195–204.

Falkowski, P.G., 1991. Species variability in the fractionation of ^{13}C and ^{12}C by marine phytoplankton. Journal of Plankton Research 13, 21–28.

Fertig, B., Carruthers, T.J.B., Dennison, W.C., Jones, A.B., Pantus, F., Longstaff, B., 2009. Oyster and macroalgae bioindicators detect elevated $\delta^{15}N$ in Maryland's coastal bays. Estuaries and Coasts 32, 773–786.

Fishelson, L., 1970. Behaviour and ecology of a population of *Abudefduf saxatilis* (Pomacentridae, Teleostei) at Eilat (Red Sea). Animal Behaviour 18, 225–237.

Fogel, M.L., Wooler, M.J., Smallwood, B.J., Roberts, Q., Romero, I., Meyers, M.J., 2008. Unusually negative nitrogen isotopic compositions ($\delta^{15}N$) of mangroves and lichens in an oligotrophic, microbially-influenced ecosystem. Biogeosciences 5, 1693–1704.

Frédérich, B., Fabri, G., Lepoint, G., Vandewalle, P., Parmentier, E., 2009. Trophic niches of thirteen damselfishes (Pomacentridae) at the Grand Récif of Toliara, Madagascar. Ichthyological Research 56, 10–17.

Froese, R., Pauly, D. (Eds.), 2013. FishBase. World Wide Web electronic publication (www.fishbase.org, version (02/2013)).

Fry, B., Wainwright, S.C., 1991. Diatom sources of ^{13}C-rich carbon in marine food webs. Marine Ecology-Progress Series 76, 149–157.

Fry, B., Lutes, R., Northam, M., Parker, P.L., Ogden, J., 1982. A $^{13}C/^{12}C$ comparison of food webs in Caribbean seagrass meadows and coral reefs. Aquatic Botany 14, 389–398.

Fukumori, K., Oi, M., Doi, H., Takahashi, D., Okuda, N., Miller, T.W., Kuwae, M., Miyasaka, H., Genkai-Kato, M., Koizumi, Y., Omori, K., Takeoka, H., 2008. Bivalve tissue as a carbon and nitrogen isotope baseline indicator in coastal ecosystems. Estuarine, Coastal and Shelf Science 79, 45–50.

Furnas, M., Mitchell, A., Skuza, M., Brodie, J., 2005. In the other 90%: phytoplankton in the Great Barrier Reef Lagoon. Marine Pollution Bulletin 51, 253–256.

Gearing, J.N., Gearing, P.J., Rudnick, D.T., Requejo, A.G., Hutchins, M.J., 1984. Isotopic variability of organic carbon in a phytoplankton-based, temperate estuary. Geochimica et Cosmochimica Acta 48, 1089–1098.

Geider, R., La Roche, J., 2002. Redfield revisited: variability of C:N:P in marine microalgae and its biochemical basis. European Journal of Phycology 37, 1–17.

Genin, A., Monismith, S.G., Reidenbach, M.A., Yahel, G., Koseff, J.R., 2009. Intense benthic grazing of phytoplankton in a coral reef. Limnology and Oceanography 54, 938–951.

Graham, B.S., Koch, P.L., Newsome, S.D., McMahon, K.W., Aurioles, D., 2010. Using isoscapes to trace the movements and foraging behavior of top predators in oceanic ecosystems. In: West, J.B., Bowen, G.J., Dawson, T.E., Tu, K.P. (Eds.), Isoscapes: Understanding Movement, Pattern, and Processes on Earth Through Isotope Mapping. Springer, Dordrecht, pp. 299–318.

Grasshoff, K., Kremling, K., Ehrhardt, M., 1999. Methods of Seawater Analysis, 3rd edn. Wiley VCH, Weinheim.

Greenwood, N.D.W., Sweeting, C.J., Polunin, N.V.C., 2010. Elucidating the trophodynamics of four coral reef fishes of the Solomon Islands using $\delta^{15}N$ and $\delta^{13}C$. Coral Reefs 29, 785–792.

Guildford, S.J., Hecky, R.E., 2000. Total nitrogen, total phosphorus, and nutrient limitation in lakes and oceans: is there a common relationship? Limnology and Oceanography 45, 1213–1223.

Håkanson, L., Bryhn, A.C., Hytteborn, J.K., 2007. On the issue of limiting nutrients and predictions of cyanobacteria in aquatic systems. The Science of the Total Environment 379, 89–108.

Halim, Y., 1984. Plankton of the Red Sea and the Arabian Gulf. Deep-Sea Research 31, 969–982.

Halsband-Lenk, C., Hirche, H.-J., Carlotti, F., 2002. Temperature impact on reproduction and development of congener copepod population. Journal of Experimental Marine Biology and Ecology 271, 121–153.

Hamilton, S.K., Sippel, S.J., Bunn, S.E., 2005. Separation of algae from detritus for stable isotope or ecological stoichiometry studies using density fractionation in colloidal silica. Limnology and Oceanography: Methods 3, 149–157.

Harmelin-Vivien, M.L., Loizeau, V., Mellon, C., Beker, B., Arlhac, D., Bodigel, X., Ferraton, F., Hermand, R., Philippon, X., Salen-Picard, C., 2008. Comparison of C and N stable isotope ratios between surface particulate organic matter and microphytobenthos in the Gulf of Lions (NW Mediterranean). Continental Shelf Research 28, 1911–1919.

Hauss, H., Franz, J.M.S., Hansen, T., Struck, U., Sommer, U., 2013. Relative inputs of upwelled and atmospheric nitrogen to the eastern tropical North Atlantic food web: spatial distribution of $\delta^{15}N$ in mesozooplankton and relation to dissolved nutrient dynamics. Deep-Sea Research Part I 75, 135–145.

Hawkins, A.J.S., Klumpp, D.W., 1995. Nutrition of the giant clam *Tridacna gigas* (L.). II. Relative contributions of filter-feeding and the ammonium–nitrogen acquired and recycled by symbiotic alga towards total nitrogen requirements for tissue growth and metabolism. Journal of Experimental Marine Biology and Ecology 190, 263–290.

Heikoop, J.M., Dunn, J.J., Risk, M.J., Tomascik, T., Schwarcz, H.P., Sandeman, I.M., Sammarco, P.W., 2000. $\delta^{15}N$ and $\delta^{13}C$ of coral tissue show significant inter-reef variation. Coral Reefs 19, 189–193.

Herzka, S.Z., 2005. Assessing connectivity of estuarine fishes based on stable isotope ratio analysis. Estuarine, Coastal and Shelf Science 64, 58–69.

Hesslein, R.H., Hallard, K.A., Ramlal, P., 1993. Replacement of sulphur, carbon and nitrogen in tissue of growing Broad Whitefish (*Coregonus nasus*) in response to a change in diet traced by $\delta^{34}S$, $\delta^{13}C$, and $\delta^{15}N$. Canadian Journal of Fisheries and Aquatic Sciences 50, 2071–2076.

Hill, J.M., McQuaid, C.D., 2008. $\delta^{13}C$ and $\delta^{15}N$ biogeographic trends in rocky intertidal communities along the coast of South Africa: evidence of strong environmental signatures. Estuarine, Coastal and Shelf Science 80, 261–268.

Hobson, K.A., 1999. Tracing origins and migration of wildlife using stable isotopes: a review. Oecologia 120, 314–326.

Hobson, K.A., Welch, H.E., 1992. Determination of trophic relationships within a high Arctic marine food web using $\delta^{13}C$ and $\delta^{15}N$ analysis. Marine Ecology-Progress Series 84, 9–18.

Iverson, S.J., 2009. Tracing aquatic food webs using fatty acids from qualitative indicators to quantitative determination. In: Arts, M.T., Brett, M.T., Kainz, M.J. (Eds.), Lipids in Aquatic Ecosystems. Springer, Dordrecht, pp. 281–307.

Jantzen, C., Wild, C., El-Zibdah, M., Roa-Quiaoit, H.A., Haacke, C., Richter, C., 2008. Photosynthetic performance of giant clams, *Tridacna maxima* and *T. squamosa*, Red Sea. Marine Biology 155, 211–221.

Jennings, S., Polunin, N.V.C., 1996. Impacts of fishing on tropical reef ecosystems. Ambio 25, 44–49.

Jennings, S., Warr, K.J., 2003. Environmental correlates of large-scale spatial variation in the $\delta^{15}N$ of marine animals. Marine Biology 142, 1131–1140.

Kaehler, S., Pakhmomov, E.A., McQuaid, C.D., 2000. Trophic structure of the marine food web at the Prince Edwards Islands (Southern Ocean) determined by $\delta^{13}C$ and $\delta^{15}N$ analysis. Marine Ecology-Progress Series 208, 13–20.

Karl, D., Michaels, A., Bergmann, B., Capone, D., Carpenter, E., Letelier, R., Lipschultz, F., Paerl, H., Sigman, D., Stal, L., 2002. Dinitrogen fixation in the world's oceans. Biogeochemistry 57 (58), 47–98.

Khalaf, M.A., Kochzius, M., 2002. Changes in trophic community structure of shore fishes at an industrial site in the Gulf of Aqaba, Red Sea. Marine Ecology-Progress Series 239, 287–299.

Khalesi, M.K., Beeftink, H.H., Wijffels, R.H., 2011. Energy budget for the cultured, zooxanthellate octocoral *Sinularia flexibilis*. Marine Biotechnology 13, 1092–1098.

Klumpp, D.W., Bayne, B.L., Hawkins, A.J.S., 1992. Nutrition of the giant clam *Tridacna gigas* (L.). I. Contribution of filter feeding, photosynthates to respiration and growth. Journal of Experimental Marine Biology and Ecology 155, 105–122.

Kolasinski, J., Rogers, K., Frouin, P., 2008. Effects of acidification on carbon and nitrogen stable isotopes of benthic macrofauna from a tropical coral reef. Rapid Communications in Mass Spectrometry 22, 2955–2960.

Kolasinski, J., Rogers, K., Cuet, P., Barry, B., Frouin, P., 2011. Sources of particulate organic matter at the ecosystem scale: a stable isotope and trace element study in a tropical coral reef. Marine Ecology-Progress Series 443, 77–93.

Krone, R., Paster, M., Schuhmacher, H., 2011. Effect of the surgeonfish *Ctenochaetus striatus* (Acanthuridae) on the process of sediment transport and deposition on a coral reef in the Red Sea. Facies 57, 215–221.

Kürten, B., Painting, S.J., Struck, U., Polunin, N.V.C., Middelburg, J.J., 2011. Tracking seasonal changes in North Sea zooplankton trophic dynamics using stable isotopes. Biogeochemistry 113, 167–187.

Kürten, B., Frutos, I., Struck, U., Painting, S.J., Polunin, N.V.C., Middelburg, J.J., 2012. Trophodynamics and functional feeding groups of North Sea fauna: a combined stable isotope and fatty acid approach. Biogeochemistry 113, 189–212.

Lamb, K., Swart, P.K., 2008. The carbon and nitrogen isotopic values of particulate organic material from the Florida Keys a temporal and spatial study. Coral Reefs 27, 351–362.

Layman, C.A., Arrington, D.A., Montana, C.G., Post, D.M., 2007. Can stable isotope ratios provide for community-wide measures of trophic structure? Ecology 88, 42–48.

Layman, C.A., Araujo, M.S., Boucek, R., et al., 2012. Applying stable isotopes to examine food-web structure: an overview of analytical tools. Biological Reviews 87, 545–562.

Lepš, J., Šmilauer, P., 2003. Multivariate Analysis of Ecological Data using CANOCO. Cambridge University Press, Cambridge.

Lesser, M.P., Falcón, L.I., Rodríguez, A., Enríquez, S., Hoegh-Guldberg, O., Iglesias-Prieto, R., 2007. Nitrogen fixation by symbiotic cyanobacteria provides a source of nitrogen for the scleractinian coral *Montastraea cavernosa*. Marine Ecology-Progress Series 346, 143–153.

Marion, G.S., Dunbar, R.B., Mucciarone, D.A., Kremer, J.N., Lansing, J.S., Arthawiguna, A., 2005. Coral skeletal δ^{15}N reveals isotopic traces of an agricultural revolution. Marine Pollution Bulletin 50, 931–944.

Mariotti, A., Lancelot, C., Billen, G., 1984. Natural isotopic composition of nitrogen as a tracer of origin for suspended organic matter in the Scheldt estuary. Geochimica et Cosmochimica Acta 48, 549–555.

Marshall, J.D., Brooks, J.R., Lajtha, K., 2007. Sources of variation in the stable isotopic composition of plants. In: Lajtha, K., Michener, R.H. (Eds.), Stable Isotopes in Ecology and Environmental Science. Blackwell Scientific Publications, London, pp. 22–60.

Marshell, A., Mumby, P.J., 2012. Revisiting the functional roles of surgeonfish *Acanthurus nigrofuscus* and *Ctenochaetus striatus*. Coral Reefs 31, 1092–1101.

Mateo, M.A., Serrano, O., Serrano, L., Michener, R.H., 2008. Effects of sample preparation on stable isotope ratios of carbon and nitrogen in marine invertebrates: implications for food web studies using stable isotopes. Oecologia 157, 105–115.

McClelland, J.W., Valiela, I., Michener, R.H., 1997. Nitrogen-stable isotope signatures in estuarine food webs: a record of increasing urbanization in coastal watersheds. Limnology and Oceanography 42, 930–937.

McClelland, J.W., Holl, C.M., Montoya, J.P., 2003. Relating low δ^{15}N values of zooplankton to N_2-fixation in the tropical North Atlantic: insights provided by stable isotope ratios of amino acids. Deep-Sea Research Part I 50, 849–861.

McCutchan Jr., J.H., Lewis Jr., W.M., Kendall, C., McGrath, C.C., 2003. Variation in trophic shift for stable isotope ratios of carbon, nitrogen, and sulfur. Oikos 102, 378–390.

McKinnon, A.D., 1996. Growth and development in the subtropical copepod *Acrocalanus gibber*. Limnology and Oceanography 41, 1439–1447.

McMahon, K.W., Hamady, L.L., Thorrold, S.R., 2013. A review of ecogeochemistry approaches to estimating movements of marine animals. Limnology and Oceanography 58, 697–714.

Mill, A.C., 2007. Stable isotope data as reef food-web descriptors in a dynamic tropical environment. (Ph.D. thesis) Newcastle University.

Minagawa, M., Wada, E., 1984. Stepwise enrichment of ^{15}N along food chains: further evidence and the relation between δ^{15}N and animal age. Geochimica et Cosmochimica Acta 48, 1135–1140.

Moberg, F., Folke, C., 1999. Ecological goods and services of coral reef ecosystems. Ecological Economics 29, 215–233.

Mohamed, Z.A., Al-Shehri, A.M., 2012. The link between shrimp farm runoff and blooms of toxic *Heterosigma akashiwo* in Red Sea coastal waters. Oceanologia 54, 287–309.

Monismith, S., Genin, A., Reidenbach, M.A., Yahel, G., Koseff, J.R., 2006. Thermally driven exchanges between a coral reef and the adjoining ocean. Journal of Physical Oceanography 36, 1332–1347.

Montoya, J.P., Carpenter, E.J., Capone, D.G., 2002. Nitrogen fixation and nitrogen isotope abundances in zooplankton of the oligotrophic North Atlantic. Limnology and Oceanography 47, 1617–1628.

Muscatine, L., Porter, J.W., Kaplan, I.R., 1989. Resource partitioning by reef corals as determined from stable isotope composition. I. δ^{13}C of zooxanthellae and animal tissue vs. depth. Marine Biology 100, 185–193.

Naumann, M.S., Richter, C., El-Zibdah, M., Wild, C., 2009. Coral mucus as an efficient trap for picoplanktonic cyanobacteria: implications for pelagic–benthic coupling in the reef ecosystem. Marine Ecology-Progress Series 385, 65–76.

Neumann, A.C., McGill, D.A., 1962. Circulation of the Red Sea in early summer. Deep-Sea Research 8, 223–235.

Newsome, S.D., Martinez del Rio, C., Bearhop, S., Phillips, D.L., 2007. A niche for isotopic ecology. Frontiers in Ecology and the Environment 5, 429–436.

Parnell, A.C., Inger, R., Bearhop, S., Jackson, A.L., 2010. Source partitioning using stable isotopes: coping with too much variation. PloS One 5, e9672. http://dx.doi.org/10.1371/journal.pone.0009672.

Patzert, W.C., 1974. Wind-induced reversal in Red Sea circulation. Deep-Sea Research 21, 109–121.

Peterson, B.J., Fry, B., 1987. Stable isotopes in ecosystem studies. Annual Review of Ecology and Systematics 18, 293–320.

Phillips, D.L., Gregg, J.W., 2003. Source partitioning using stable isotopes: coping with too many sources. Oecologia 136, 261–269.

Pinnegar, J.K., Polunin, N.V.C., 1999. Differential fractionation of δ^{13}C and δ^{15}N among fish tissues: implications for the study of trophic interactions. Functional Ecology 13, 225–231.

Pinnegar, J.K., Polunin, N.V.C., 2000. Contributions of stable-isotope data to elucidating food webs of Mediterranean rocky littoral fishes. Oecologia 122, 399–409.

Polunin, N.V.C., Harmelin-Vivien, M.L., Galzin, R., 1995. Contrasts in algal food processing among five herbivorous coral-reef fishes. Journal of Fish Biology 47, 455–465.

Polunin, N.V.C., Morales-Nin, B., Pawsey, W.E., Cartes, J.E., Pinnegar, J.K., Moranta, J., 2001. Feeding relationships in Mediterranean bathyal assemblages elucidated by stable nitrogen and carbon isotope data. Marine Ecology-Progress Series 220, 13–23.

Post, D.M., 2002. Using stable isotopes to estimate trophic position: models, methods, and assumptions. Ecology 83, 703–718.

Raikov, D.F., Hamilton, S.K., 2001. Bivalve diets in a midwestern U.S. stream: a stable isotope enrichment study. Limnology and Oceanography 46, 514–522.

Raitsos, D.E., Pradhan, Y., Brewin, R.J.W., Stenchikov, G., Hoteit, I., 2013. Remote sensing the phytoplankton seasonal succession of the Red Sea. PloS One 8, e64909. http://dx.doi.org/10.1371/journal.pone.0064909.

Randall, J.E., Ben-Tuvia, A., 1983. A review of the groupers (Pisces: Serranidae: Epinephelinae) of the Red Sea, with description of a new species of *Cephalopholis*. Bulletin of Marine Science 33, 373–426.

Rau, G.H., Riebesell, U., Wolf-Gladrow, D., 1996. A model of photosynthetic ^{13}C fractionation by marine phytoplankton based on diffusive molecular CO_2 uptake. Marine Ecology-Progress Series 133, 275–285.

R Core Team, 2013. R: A language and environment for statistical computing. R Foundation for Statistical Computing, Vienna, Austria. ISBN 3-900051-07-0, URL http://www.R-project.org/.

Risk, M.J., Lapointe, B.E., Sherwood, O.A., Bedford, B.J., 2009a. The use of δ^{15}N in assessing sewage stress on coral reefs. Marine Pollution Bulletin 58, 793–802.

Risk, M.J., Sherwood, O.A., Nairn, R., Gibbons, C., 2009b. Tracking the record of sewage discharge off Jeddah, Saudi Arabia, since 1950, using stable isotope records from antipatharians. Marine Ecology-Progress Series 397, 219–226.

Savage, C., 2005. Tracing the influence of sewage nitrogen in a coastal ecosystem using stable nitrogen isotopes. Ambio 34, 145–150.

Schell, D.M., Barnett, B.A., Vinette, K.A., 1998. Carbon and nitrogen isotope ratios in zooplankton of the Bering, Chukchi and Beaufort seas. Marine Ecology-Progress Series 162, 11–23.

Schimmelmann, A., Albertino, A., Sauer, P.E., Qi, H., Molinie, R., Mesnard, F., 2009. Nicotine, acetanilide and urea multi-level ^{2}H, ^{13}C- and ^{15}N-abundance reference materials for continuous-flow isotope ratio mass spectrometry. Rapid Communications in Mass Spectrometry 23, 3513–3521.

Shpigel, M., Fishelson, L., 1989a. Food habits and prey selection of three species of groupers from the genus *Cephalopholis* (Serranidae: Teleostei). Environmental Biology of Fishes 24, 67–73.

Shpigel, M., Fishelson, L., 1989b. Habitat partitioning between species of the genus *Cephalopholis* (Pisces, Serranidae) across the fringing reef of the Gulf of Aqaba (Red Sea). Marine Ecology-Progress Series 58, 17–22.

Sigman, D.M., Altabet, M.A., McCorkle, D.C., Francois, R., Fischer, G., 2000. The δ^{15}N of nitrate in the Southern Ocean: nitrogen cycling and circulation in the ocean interior. Journal of Geophysical Research Oceans 105, 19599–19614.

Slattery, M., Gochfeld, D.J., Easson, C.G., O'Donahue, L.R.K., 2013. Facilitation of coral reef biodiversity and health by cave sponge communities. Marine Ecology-Progress Series 476, 71–86.

Sofianos, S.S., Johns, W.E., 2007. Observation of the Red Sea circulation. Journal of Geophysical Research 112, 1–20.

Sommer, U., Stibor, H., Katechakis, A., Sommer, F., Hansen, T., 2002. Pelagic food web configurations at different levels of nutrient richness and their implications for the ratio fish production:primary production. Hydrobiologia 484, 11–20.

Soreide, J.E., Tamelander, T., Hop, H., Hobson, K.A., Johansen, I., 2006. Sample preparation effects on stable C and N isotope values: a comparison of methods in Arctic marine food web studies. Marine Ecology-Progress Series 328, 17–28.

Sweeting, C.J., Jennings, S., Polunin, N.V.C., 2005. Variance in isotopic signatures as a descriptor of tissue turnover and degree of omnivory. Functional Ecology 19, 777–784.

Sweeting, C.J., Barry, J., Barnes, C., Polunin, N.V.C., Jennings, S., 2007. Effects of body size and environment on diet-tissue δ^{15}N fractionation in fishes. Journal of Experimental Marine Biology and Ecology 340, 1–10.

van Duyl, F.C., Moodley, L., Nieuwland, G., van Ijzerloo, L., van Soest, R.W.M., Houtekamer, M., Meesters, E.H., Middelburg, J.J., 2011. Coral cavity sponges depend on reef-derived food resources: stable isotope and fatty acid constraints. Marine Biology 158, 1653–1666.

Vander Zanden, M.J., Cabana, G., Rasmussen, J.B., 1997. Comparing trophic position of freshwater fish calculated using stable nitrogen isotope ratios (δ^{15}N) and literature dietary data. Canadian Journal of Fisheries and Aquatic Sciences 54, 1142–1158.

Vizzini, S., Mazzola, A., 2006. The effects of anthropogenic organic matter inputs on stable carbon and nitrogen isotopes in organisms from different trophic levels in a southern Mediterranean coastal area. The Science of the Total Environment 368, 723–731.

Vollenweider, R.A., Kerekes, J., 1982. Eutrophication of waters. Monitoring Assessment and Control. OECD Cooperative Program on Monitoring of Inland Waters (Eutrophication Control), Environment Directorate. OECD, Paris 1–154.

Wankel, S.D., Chen, Y., Kendall, C., Post, A.F., Paytan, A., 2010. Sources of aerosol nitrate to the Gulf of Aqaba: evidence from δ^{15}N and δ^{18}O of nitrate and trace metal chemistry. Marine Chemistry 120, 90–99.

Wild, C., Huettel, M., Klueter, A., Kremb, S.G., Rasheed, M.Y.M., Jørgensen, B.B., 2004. Coral mucus functions as an energy carrier and particle trap in the reef ecosystem. Nature 428, 66–70.
Wyatt, A.S.J., Lowe, R.J., Humphries, S., Waite, A.M., 2010a. Particulate nutrient fluxes over a fringing coral reef: relevant scales of phytoplankton production and mechanisms of supply. Marine Ecology-Progress Series 405, 113–130.
Wyatt, A.S.J., Waite, A.M., Humphries, S., 2010b. Variability in isotope discrimination factors in coral reef fishes: implications for diet and food web reconstruction. PloS One 5, e13682. http://dx.doi.org/10.1371/journal.pone.0013682.
Wyatt, A.S.J., Falter, J.L., Lowe, R.J., Humphries, S., Waite, A.M., 2012a. Oceanographic forcing of nutrient uptake and release over a fringing coral reef. Limnology and Oceanography 57, 401–419.
Wyatt, A.S.J., Waite, A.M., Humphries, S., 2012b. Stable isotope analysis reveals community-level variation in fish trophodynamics across a fringing reef. Coral Reefs 31, 1029–1044.
Wyatt, A.S.J., Lowe, R.J., Humphries, S., Waite, A.M., 2013. Particulate nutrient fluxes over a fringing coral reef: source-sink dynamics inferred from carbon and nitrogen ratios of stable isotopes. Limnology and Oceanography 58, 409–427.
Yahel, G., Post, A.F., Fabricius, M., Vaulot, D., Genin, A., 1998. Phytoplankton distribution and grazing near coral reefs. Limnology and Oceanography 43, 551–563.
Yamamuro, M., Kayanne, H., Minagawa, M., 1995. Carbon and nitrogen stable isotopes of primary producers in coral reef ecosystems. Limnology and Oceanography 40, 617–621.